1990

Peak analysis in gas chromatography and the development of new stationary phases for anion chromatography

Roy Francis Strasburg
Iowa State University

Order Number 9101380

Peak analysis in gas chromatography and the development of new stationary phases for anion chromatography

Strasburg, Roy Francis, Ph.D.

Iowa State University, 1990

U·M·I
300 N. Zeeb Rd.
Ann Arbor, MI 48106

Peak analysis in gas chromatography and the development of new stationary phases for anion chromatography

by

Roy Francis Strasburg

A Dissertation Submitted to the

Graduate Faculty in Partial Fulfillment of the

Requirements for the Degree of

DOCTOR OF PHILOSOPHY

Department: Chemistry
Major: Analytical Chemistry

Approved:

Signature was redacted for privacy.

In Charge of Major Work

Signature was redacted for privacy.

For the Major Department

Signature was redacted for privacy.

For the Graduate College

Iowa State University
Ames, Iowa

1990

TABLE OF CONTENTS

GENERAL INTRODUCTION

During the past several years, many improvements have been made in gas and ion-exchange chromatography. One area of continued interest is in the reduction of analysis time and in the improvement of chromatographic efficiency. Contributions in these areas require an understanding of basic chromatographic principles. It is the aim of this work to explore these principles and apply them towards improving chromatographic separations.

In open-tubular, gas chromatography, there are three contributions to the total width of a chromatographic peak, or band, namely band-spreading due to axial diffusion, resistance to mass transfer, and extra-column band spreading.

Band spreading due to these three phenomenon is described by the Golay equation. Band spreading due to axial diffusion occurs as a sample transverses the chromatographic column and the sample molecules in the gas phase diffuse from a higher concentration to a lower concentration. Band spreading due to resistance to mass transfer is due to the different rates at which the molecules of a sample partition between the mobile phase

and the stationary phase. The third phenomenon, extra-column band broadening, occurs outside the chromatographic column. For example, pressure surges in the injection port, the void volume in the detector, or the time required to make an injection, all contribute to the extra-column band broadening.

In Section I, the effect of a diluent on the total band width of a chromatographic peak is investigated. With the interest in reduction of analysis time, very early eluting peaks must be as narrow as possible. It is shown that when a diluent is present in a liquid sample, the peaks are broader than when the diluent is absent. This is attributed to the rapid vaporization of the sample in the injection port, which creates chaotic conditions. A pressure surge is produced, which is transmitted to the column, producing an increase in extra-column band broadening. By selecting the proper sample conditions, it is shown that the extra-band broadening can be significantly reduced, thus increasing the overall efficiency of the chromatographic separation.

One fundamental quantity in gas chromatography that needs to be known precisely is the gas hold-up time, or dead time (t_M), of the capillary column. The dead time is the time required for an unretained sample to transverse

the chromatographic column. Typically, the retention time of methane is used. However, methane is significantly retained on the column resulting in an incorrect value for t_M. Inert gases, such as nitrogen, which are not retained, do not produce a response with a flame ionization detector.

The correct t_M value is necessary in calculating correct values for the capacity factor, Kovats' indices, and carrier gas flow rate. Many attempts have been made to solve this problem mathematically. These methods can be divided into two general approaches; an iterative method and a statistical method. Unfortunately, these methods have been shown to be inadequate, either because they are unnecessarily complex or simply inaccurate.

Section II presents a simple, precise and rapid method to determine t_M mathematically. An iterative approach is used which takes advantage of a popular programmable calculator. A second method, developed by Dr. Dan Scott, is also described for completeness. The effects of temperature, flow rate and split ratio on t_M are investigated. These two methods are compared to previously published methods to show their validity. Finally, a simple method for calculating Kovats' indices is presented using the correct value for t_M.

Inorganic anions are now routinely analyzed by anion-exchange chromatography. Quantitative and qualitative information is obtained from peak area (or height) and the analyte's retention time. However, in single-column, anion-exchange chromatography, the first baseline perturbation is the injection peak, which may be observed as a traditional peak or as a baseline dip. This injection peak contains the cations associated with the salt sample that was injected. With proper sample treatment, the injection peak can be a rich source of information.

Section III presents a novel method of determining quantitatively the cations present in a salt mixture, using the information provided by the injection peak and the analyte peaks. The sample is prepared so that it contains the same concentration and pH value of the eluent ions as the mobile phase. The result is a positive injection peak, the size of which depends on the type and concentration of the cation present. The cationic content of a salt mixture is quantitatively determined in acidic, neutral, and alkaline solutions using this method. The method is shown to be simple, precise, and accurate.

Section IV describes a new anion-exchange resin suitable for anion chromatography. Small latex particles, which have been functionalized with quaternary ammonium

groups, are hydrophobically adsorbed onto non-porous, spherical, polystyrene beads. Several advantages are described, including selectivity, sensitivity, and stability. Due to the low capacity of this resin, excellent limits of detection are possible.

SECTION I. EFFECT OF SAMPLE DILUENTS ON PEAK BROADENING IN GAS CHROMATOGRAPHY

INTRODUCTION

In gas chromatography, the final peak shape of an analyte is determined by various processes the analyte undergoes from the point of injection to detection. The first step in any chromatographic separation is sample introduction. The initial treatment and mode of sample introduction determines the minimum peak width obtainable, since other processes that occur during the separation and detection will broaden the peak further. Therefore, careful attention needs to be given to the introduction of the sample into a chromatographic system.

It is a common practice in gas chromatography to use a solvent to dissolve a solid sample or to dilute a liquid sample prior to injection. Dilution is typically require in capillary gas chromatography to prevent column overloading. Column overloading results in peak distortion and a reduction in the efficiency of the capillary column [1,2].

One method of sample introduction which alleviates the problem of column overloading is the use of a vaporizing injector which splits the sample. The majority of the sample goes to waste, while only a small portion, typically two percent or less, enters the column.

With vaporizing injectors, Grob and Neukom [3] have pointed out that the rapidly vaporizing solvent creates a pressure wave that results in fairly chaotic conditions at the column inlet. They studied the impact of this effect on the split ratio and discrimination of sample components. Grob and co-workers have also studied extensively the effects of solvents in splitless capillary gas chromatography [4-9]. Miller and Jennings [10] describe the effect of a "solvent envelope" in split injection.

Using samples diluted with pentane of acetone in conjunction with a vaporizing injector and a splitter, we found the peak widths of sample components having a fairly low capacity ratio (k') to be appreciatively broader than the same peaks when an undiluted liquid sample was injected. This prompted the present investigation on the effect of a diluent for liquid samples at different split ratios and on the comparative broadening of liquid and gaseous samples.

EXPERIMENTAL

A Hewlett-Packard 5880A gas chromatograph in the split injection mode was used with a flame ionization detector. A 12.25 m x 0.20 mm i.d. J&W DB-1, crosslinked methyl-silicone capillary column was used that had a film thickness of 0.33 μm. The helium carrier gas was maintained at a linear flow rate of 47.3 cm/s for all chromatographic runs, unless otherwise noted. The chromatograms were all run isothermally at 80° C.

Injections were made manually. The injection port was maintained at 250° C. It contained a 78.5 mm x 3.9 mm i.d. glass liner packed with 80/100 mesh, 3% methyl-silicone resin, held in place by silanized glass wool.

Split ratios ranged from 40:1 to 428:1. The inlet pressure, P_i, was adjusted to maintain a constant average carrier gas flow rate of 47.3 cm/s at the various split ratios. Day-to-day variations in atmospheric pressure caused some changes in the P_i needed to maintain a constant flow rate.

The neat liquid samples were prepared by combining 20 μl each of the five C_6-C_{10} n-alkanes. The gaseous samples were prepared by mixing approximately 1.0, 3.6, 10.3, 28.8, and 56.4 μl of n-hexane, heptane, octane, nonane, and

decane, respectively, and allowing the liquid and gas phases to reach equilibrium in a vial sealed with a septum so that a 5 μl injection of the headspace sample gave approximately the same peak area for all five components.

Diluted liquid samples were prepared by adding 25 μl of pentane to 5 μl of the neat liquid sample of the C_6-C_{10} n-alkanes. Very small liquid sample volumes (0.04 μl) were injected to avoid column overloading, especially at the lower split ratios. Consistent injections of 0.04 μl samples were made with a 1.0 μl, #7101 Hamilton syringe by drawing a small amount of air into the syringe before and after the liquid sample to prevent vaporization of the sample in the needle.

The capacity ratio, k', for each peak was calculated from the retention time and the column dead time, t_M, which was 25.9 s for all chromatograms. Conditions were chosen so that the k' values of the sample compounds would be low. Typical values of k' for the n-alkanes were as follows: C_6 = 0.26, C_7 = 0.56, C_8 = 1.16, C_9 = 2.39, C_{10} = 4.84.

Widths of the chromatographic peaks were measured at one-half peak height ($w_{1/2}$) at a chart speed of 32 cm/min using a 0.05 mm Mitutoyo caliper. Peak variances (σ^2_{meas}) were calculated from $w_{1/2}$; each variance used was the average of three separate chromatographic runs.

Giddings' method [11] was used to calculate $\bar{D}_g$ for each sample compound at the average column pressure, $\bar{P}$ (typically 1.66 atm). Typical values for $\bar{D}_g$ (in cm^2/s) for the n-alkanes were: C_6 = 0.214, C_7 = 0.197, C_8 = 0.184, C_9 = 0.172, C_{10} = 0.163.

RESULTS AND DISCUSSION

Theory

It is common practice to consider various contributions to plate height in chromatography (12-16). An effort has also been made at estimating the extra-column contribution to total band broadening (17-19). However, estimating the extra column contribution is frequently inaccurate due to the assumptions that must be made.

Instead of using plate height or estimating various contributions, peak variance in time units (s^2) was used because it can be measured directly from a chromatogram. The major contributions to peak variance can be given as:

$$\sigma^2_{meas} = \sigma^2_{d} + \sigma^2_{mt} + \sigma^2_{ec} \qquad (1)$$

where σ^2_{meas} is the variance of a peak measured directly from the chromatogram; σ^2_{d}, σ^2_{mt}, and σ^2_{ec} are the variances due to axial diffusion, resistance to mass transfer, and extra-column effects, respectively.

An equation for the σ^2_{d} can be obtained from the B-term of the Golay equation after using the basic definition of plate height to convert the proper units.

$$\sigma^2_d = \frac{2D_{g(o)}L}{u_o} \cdot \frac{(1+k')^2}{\bar{u}^2} = \frac{2\bar{D}_g L(1+k')^2}{\bar{u}^3} \qquad (2)$$

where σ^2 is in s^2, $\bar{D}_g$ is the diffusion coefficient (cm^2/s), $\bar{u}$ is the linear flow rate (cm/s), and k' is the capacity ratio of a sample compound. The subscript, o, refers to the column outlet and bar terms to the average over the column length. $\bar{D}_g$ can be calculated to ±5% from structural parameters, temperature and pressure, thus permitting calculation of σ^2_d according to equation (2).

Subtracting σ^2_d from σ^2_{meas} gives $(\sigma^2_{mt} + \sigma^2_{ec})$ for each peak in the chromatogram. The factors contributing to σ^2_{mt} are contained in the C-term of the Golay equation. For thin-film capillary columns under our experimental conditions, the contributions of the C_1 term is only 1 to 2% of the C_g term. We therefore considered only the C_g term which, with an appropriate conversion to time units, gives the following:

$$\sigma^2_{mt} = \frac{L(1+6k'+11k'^2)r^2\bar{u}}{24(1+k')\bar{D}_g} \cdot \frac{(1+k')^2}{\bar{u}^2} \qquad (3)$$

where r is the inside radius of the column [20]. For a given column at fixed flow rate, equation (3) assumes the form:

$$\sigma^2_{mt} = \frac{a(1+6k'+11k'^2)}{\bar{D}_g} \qquad (4)$$

A plot of $(\sigma^2_{mt} + \sigma^2_{ec})$ against $(1+6k'+11k'^2)/\bar{D}_g$ should give a linear plot with slope of "a" and intercept = σ^2_{ec}. The effect of various modes of injection peak variance can thus be deduced by measuring σ^2_{ec} under different experimental conditions.

Neat Samples

Undiluted liquid samples containing C_6 to C_{10} n-alkanes were chromatographed at a fixed temperature and flow rate. Various split ratios were used, ranging from 40:1 to 428:1. Figure 1 shows a typical separation of these alkanes at a split ratio of 80:1. A chart speed of 32 cm/min was used to reduce the relative error in measuring the peaks' width at half height. As can be seen, the peaks are narrow and approach a gaussian distribution. The inset in Figure 1 is the same separation at a typical chart speed of 1 cm/min.

The variance of each peak was measured and the average of three chromatographic runs was taken. After subtracting the calculated variance due to axial diffusion [eq. (2)], the resulting variance was plotted against $(1+6k'+11k'^2)/\bar{D}_g$. In every instance, a linear plot was obtained with an excellent correlation coefficient for the

Figure 1. Separation of neat mixture of n-hexane, n-heptane, n-octane, n-nonane, and n-decane. Column: 12.25 m x 0.20 mm i.d. DB-1. Temperature: 80° C. Split Ratio: 80:1. Chart Speed: 32 cm/min. Insert: Chart speed of 1 cm/min

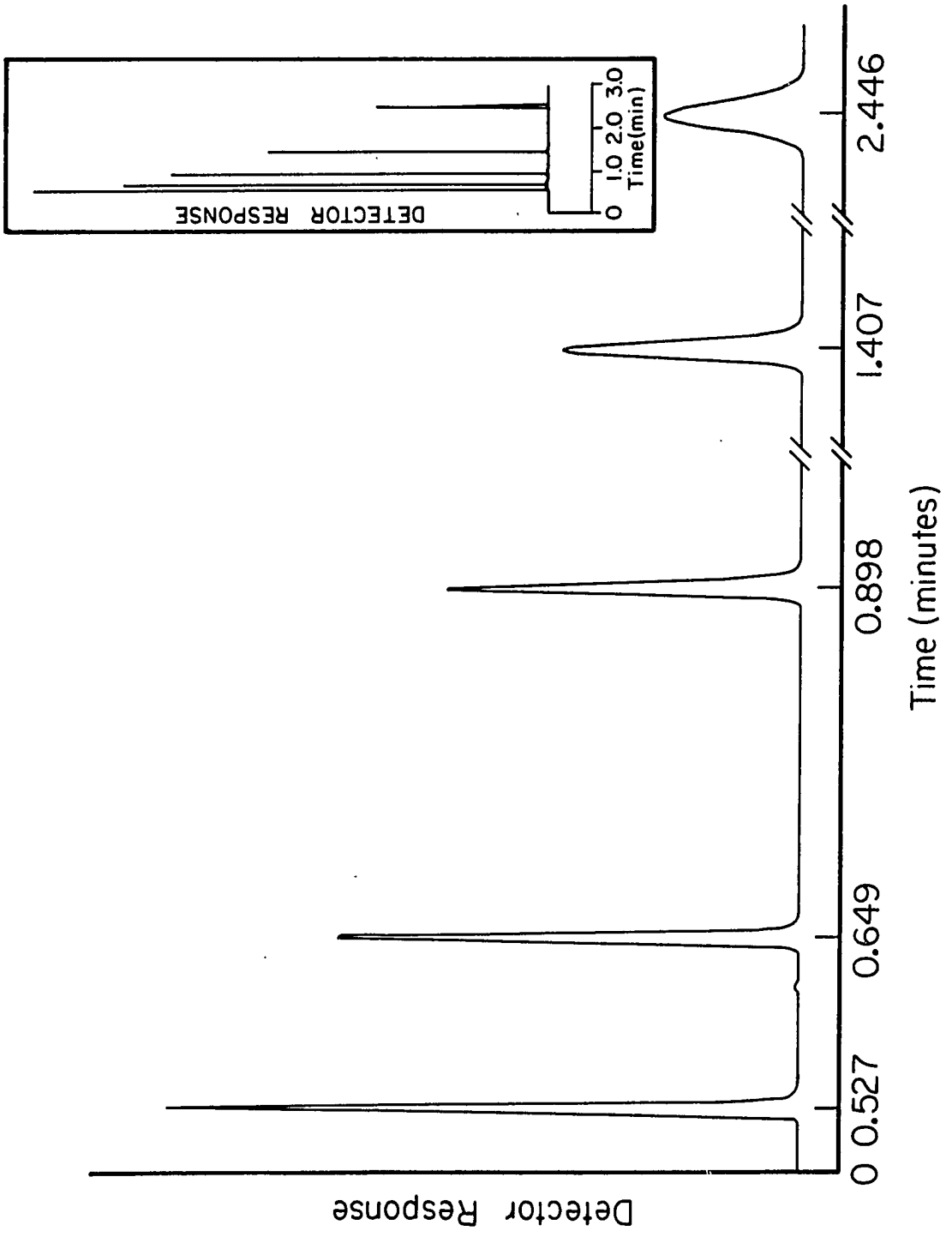
Detector Response
0 0.527
0.649
0.898
1.407
2.446
Time (minutes)
DETECTOR RESPONSE
0 1.0 2.0 3.0
Time(min)

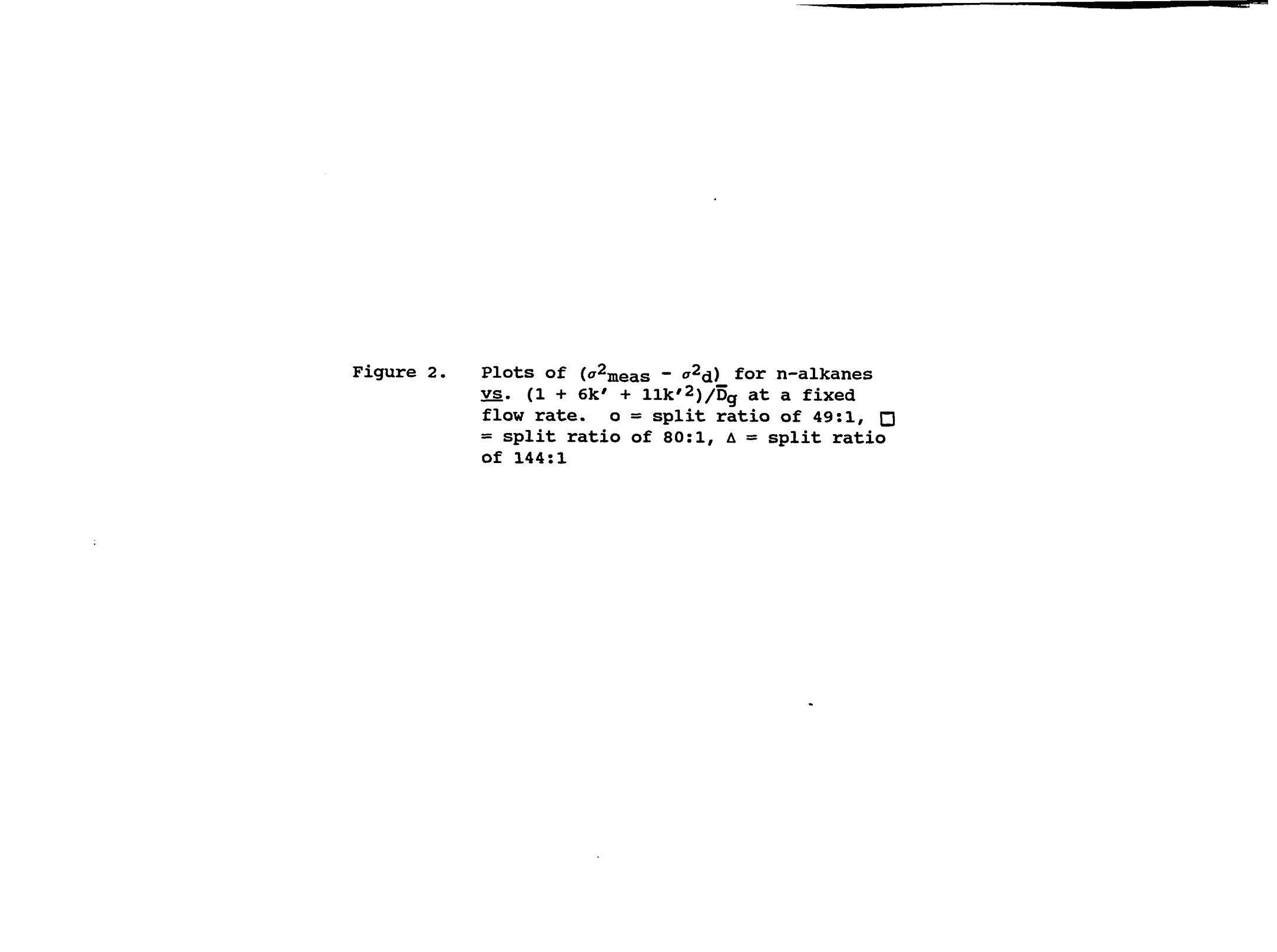

Figure 2. Plots of $(\sigma^2_{meas} - \sigma^2_d)$ for n-alkanes vs. $(1 + 6k' + 11k'^2)/\bar{D}_g$ at a fixed flow rate. o = split ratio of 49:1, □ = split ratio of 80:1, Δ = split ratio of 144:1

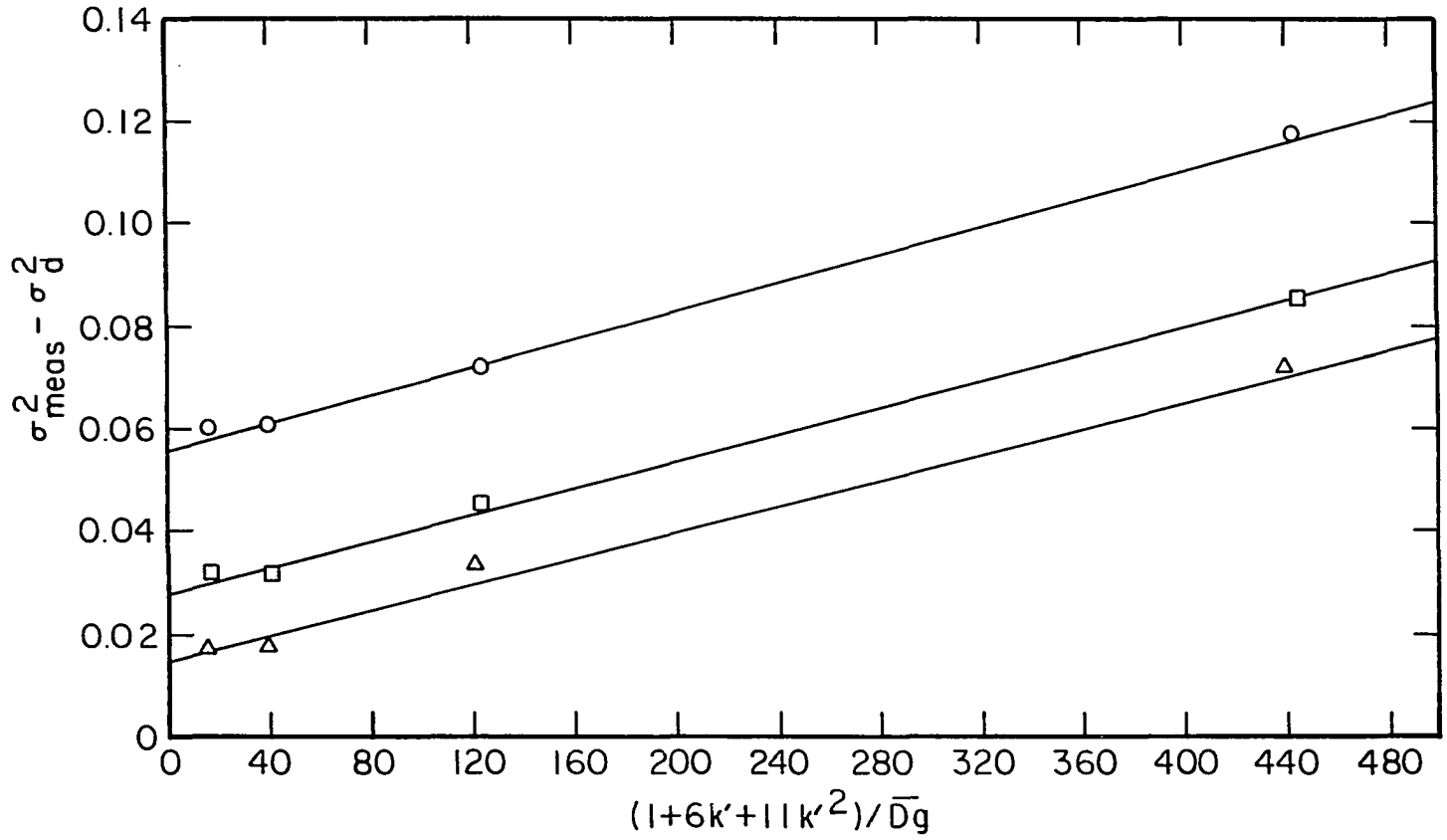
0.14
0.12
0.10
0.08
0.06
0.04
0.02
0
$\sigma^2_{meas} - \sigma^2_d$
0
40
80
120
160
200
240
280
320
360
400
440
480
$(1+6k'+11k'^2)/\overline{Dg}$

linear regression (usually 0.9996 to 1.0000). The first four points for typical plots are shown in Figure 2.

The slopes of numerous plots of this type averaged 1.32×10^{-4} with a relative standard deviation of only 4.7%. However, the intercept on the Y axis varied with the split ratio. The intercept of each plot (σ^2_{ec}) was then plotted as a function of split ratio in Figure 3. The individual points on this curve show that the reproducibility of this method is good, and also that the extra-column contribution to peak variance is much larger at the lower split ratios.

Dilute Samples

The liquid hydrocarbon samples were diluted 1:6 by volume with n-pentane and the previous experiment was repeated under identical conditions as before. Figure 4 shows a typical chromatogram of the diluted alkanes. The early peaks are broader than the same peaks in Figure 1.

Plots of the measured variance minus the variance due to axial diffusion versus $(1+6k'+11k'^2)/\bar{D}_g$ were again linear, as in Figure 2, with excellent correlation coefficients. The slopes were essentially identical with the undiluted samples. However, the values of σ^2_{ec} were distinctly higher for the samples diluted with pentane, except at the lowest split ratios (see Figure 3).

Figure 3. Effect of split ratio on extra-column variance. o = neat liquid alkanes, □ = liquid alkanes diluted 1:6 with n-pentane

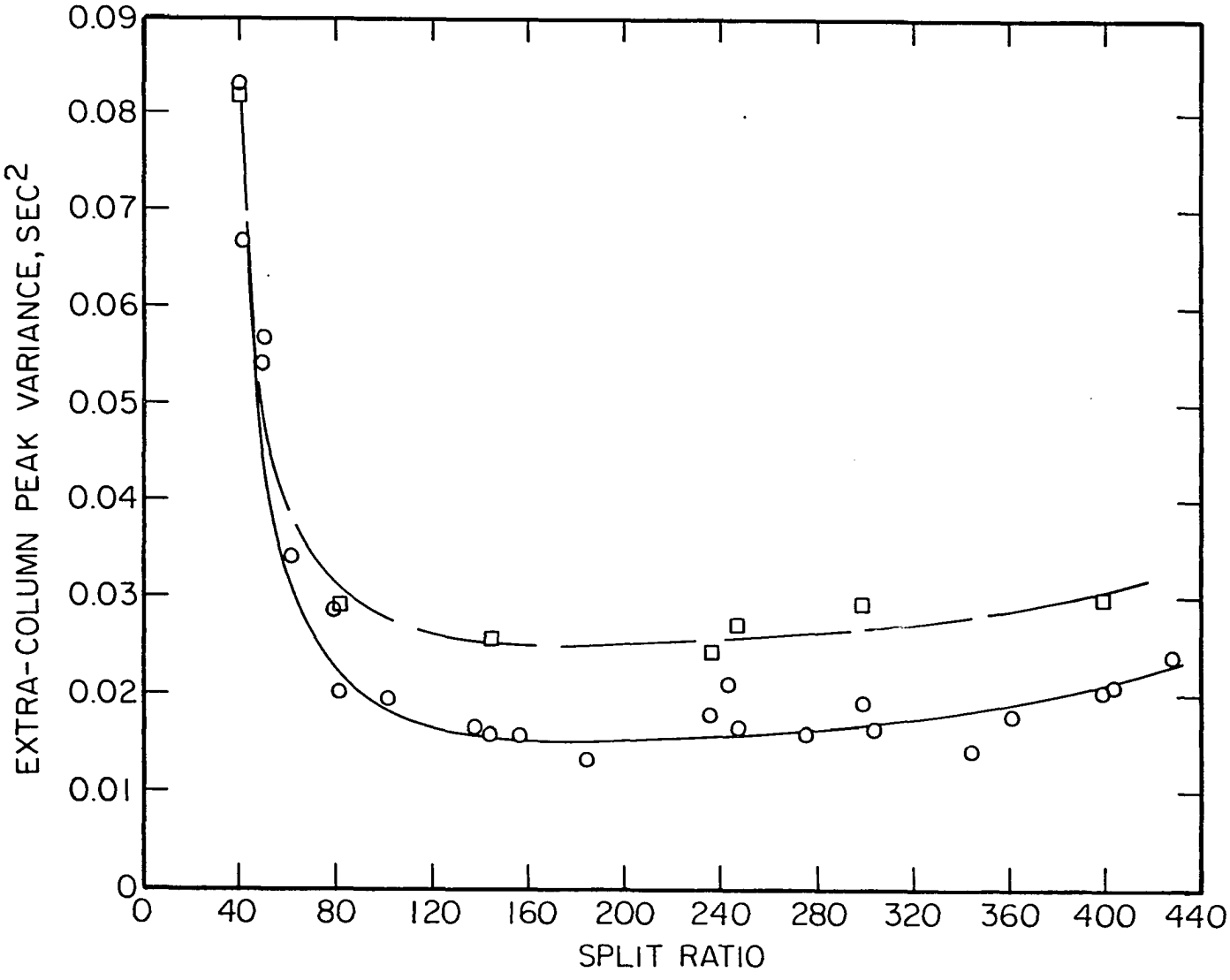
EXTRA-COLUMN PEAK VARIANCE, SEC^2
0.09
0.08
0.07
0.06
0.05
0.04
0.03
0.02
0.01
0
0
40
80
120
160
200
240
280
320
360
400
440
SPLIT RATIO

Figure 4. Separation of n-alkanes diluted 1:6 with n-pentane under the same conditions as Figure 1

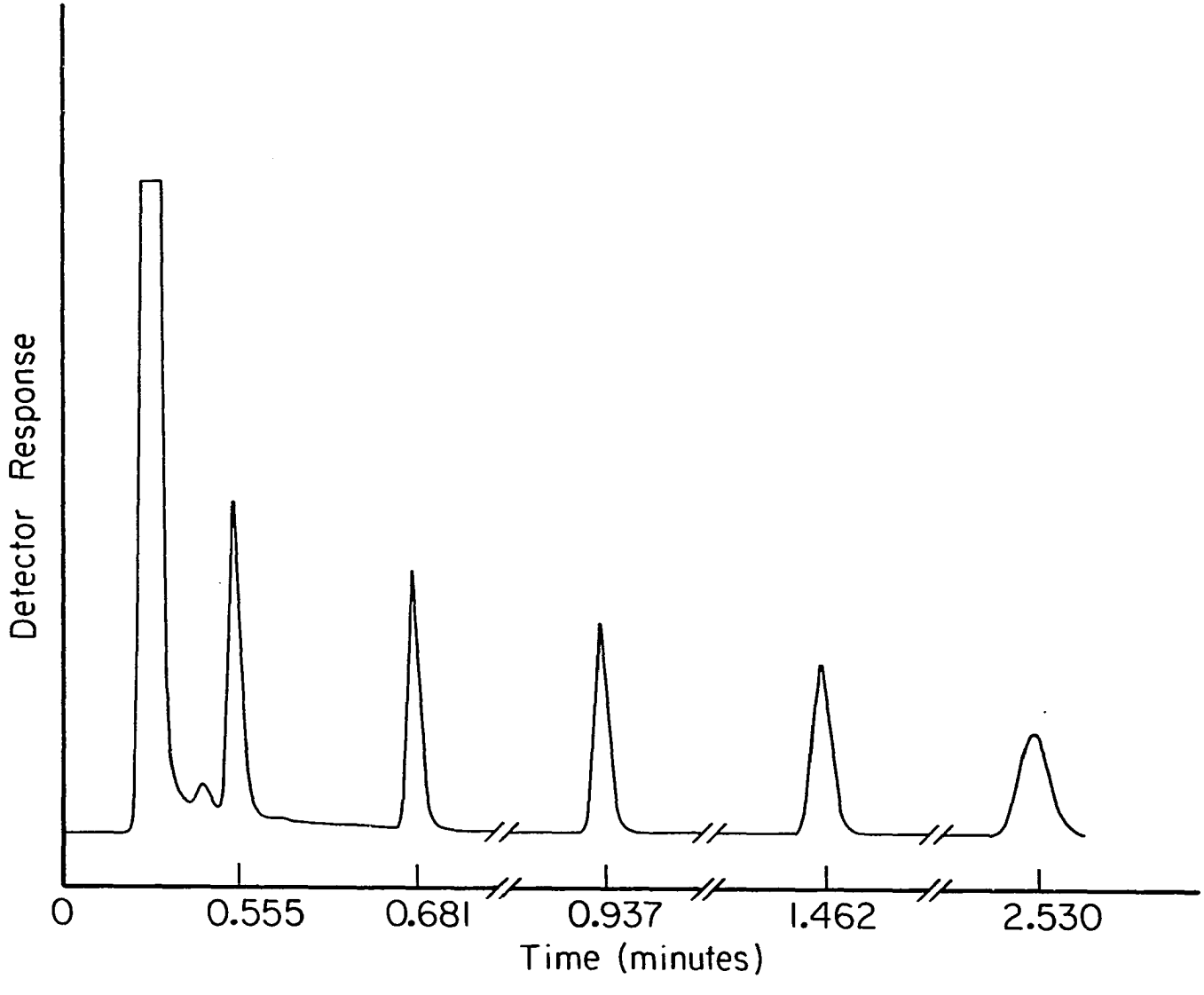
Detector Response
0
0.555
0.681
0.937
1.462
2.530
Time (minutes)

Individual peaks (such as the C_6 and C_7 peaks) were also consistently broader for the diluted samples than for the undiluted samples measured at the same split ratio. In other experiments broadening of the earlier peaks was shown to increase as the amount of pentane dilution was increased. Earlier experiments also showed that dilution of liquid samples of n-alkanes and methylketones with acetone caused broadening of the earlier peaks.

Pre-vaporized Samples

Injections of pre-vaporized, or headspace, samples containing C_6 to C_{10} n-alkanes were also made. The liquid samples of n-alkanes were allowed to equilibrate with air or an inert gas in a sealed vial. Portions of the headspace were then injected at various split ratios and the alkanes were separated under the same chromatographic conditions used for the liquid samples. The values of σ^2_{ec} were obtained graphically as before and plotted against split ratio. The values of σ^2_{ec} lie just slightly below those for neat liquid samples (Figure 5) for split ratios between 80:1 and 360:1. At a split ratio of 40:1, σ^2_{ec} for the gaseous sample is only 0.02 s^2, which is far lower than the neat liquid sample at the same split ratio.

A few experiments were performed with headspace samples of alkanes diluted with large amounts of pentane.

Figure 5. Effect of split ratio on extra-column variance. o = neat liquid alkanes, □ = prevaporized alkanes

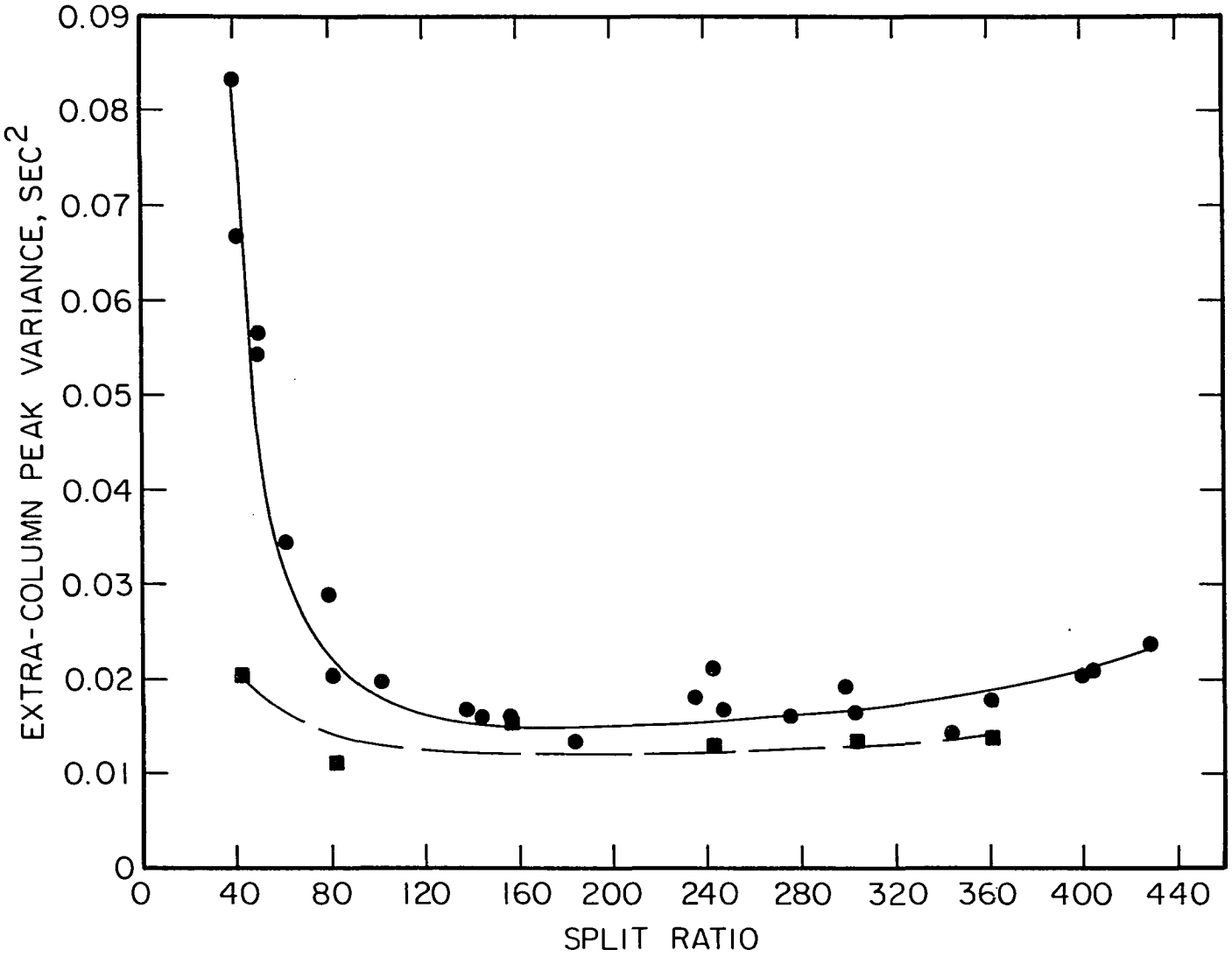
EXTRA-COLUMN PEAK VARIANCE, SEC^2
0.09
0.08
0.07
0.06
0.05
0.04
0.03
0.02
0.01
0
0
40
80
120
160
200
240
280
320
360
400
440
SPLIT RATIO

These experiments showed no additional peak broadening from the pentane. Figure 6 shows that even for early eluting peaks, peak widths for neat samples and samples containing up to 90% pentane as the diluent were identical.

Discussion

The chaotic conditions created by vaporizing liquid samples during injection, described by Grob and Neukam [3], would account for the broadening effects noted above. It also seems likely that the very volatile diluent, such as pentane, would add to the vaporizing thrust and further increase the peak broadening. The lower extra-column peak variance with gaseous samples is explained by the lack of any appreciable pressure surge during injection.

The sharp increase in extra-column variance at low split ratios, (Figures 2 and 4), is worth noting. More of the surge from rapid vaporization is apparently transmitted to the column inlet than when the split ratio is higher. Minor changes in the sample volume injected showed no trend and no substantial changes in peak variances.

It should be emphasized that these broadening effects are rather small and will only have a noticeable effect on peak width when the value of k′ is less than approximately

Figure 6. Effect of n-pentane, as a diluent, on the peak width of n-alkanes in prevaporized samples. Split Ratio: 80:1

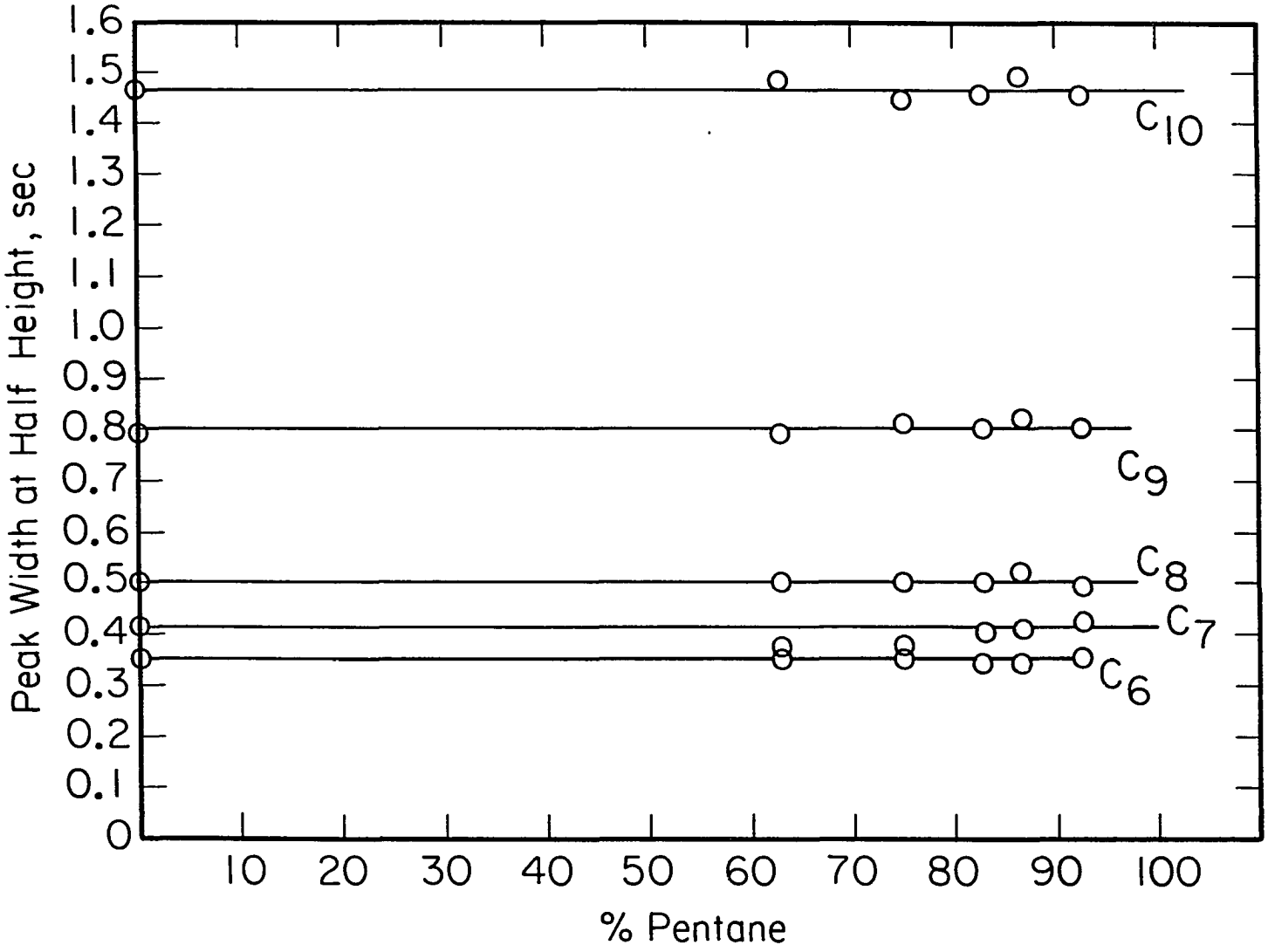
Peak Width at Half Height, sec
1.6
1.5
1.4
1.3
1.2
1.1
1.0
0.9
0.8
0.7
0.6
0.5
0.4
0.3
0.2
0.1
0
10
20
30
40
50
60
70
80
90
100
% Pentane
C10
C9
C8
C7
C6

Table I. Contribution to Total Band Variance of the Various Components (sec^2)

C	k′	σ^2_{meas}	σ^2_d		σ^2_{mt}		σ^2_{ec}	
8	0.30	0.027	0.0078	29%	0.0016	5.9%	0.0176	65%
9	0.50	0.029	0.0099	34	0.0015	5.2	0.0176	61
10	0.86	0.038	0.014	36	0.0067	18	0.0176	46
11	1.47	0.059	0.0240	41	0.017	29	0.0176	30
12	2.51	0.116	0.0462	40	0.052	45	0.0176	15
13	4.27	0.250	0.0997	40	0.132	53	0.0176	7
14	7.25	0.633	0.235	37	0.380	60	0.0176	3

Temp = 130° C
t_M = 23.15 sec
Split Ratio = 250:1

1.0 to 2.0. As can be seen in Table I, σ^2_{ec} is a significant contribution to the total variance when k′ is less than 2.5. Moreover, when k′ is less than 1.0, σ^2_{ec} is the major contribution to the total variance.

CONCLUSION

This work emphasizes the importance of several aspects of sample introduction, such as split ratio, the presence of a diluent, and sample phase, on the total peak variance in capillary gas chromatography. These aspects are shown to contribute to the extra-column variance in a vaporizing injector. A reduction in analysis time implies a reduction of the analytes' k' values. It is at these low k' values that peak variance due to extra-column band broadening is significant.

It has been shown that the use of a low split ratio or the presence of a diluent increases extra-column variance. This effect is minimized when a high split ratio (greater than 80:1) and a neat sample is injected. It was also shown that pre-vaporized, or head-space, samples produced the most narrow bands. Since the sample does not need to be vaporized in the injection port, the pressure surge caused by vaporization is eliminated.

Finally, the importance of controlling extra-column band broadening was shown to be important. When k' values are low, extra-column band broadening is shown to be a significant contribution to the total peak variance. Injections of neat or pre-vaporized samples at a high

split ratio can reduce the total variance of a early eluting analyte by as much as 50%. This will lead to well resolved peaks in the first few minutes of a chromatographic separation.

REFERENCES

1. Pretorius, W.; Lawson, K.; Bertsch, W. HRC&CC 1983, 7, 185.

2. Cardot, P.; Ignatiadis, I.; Jaulmes, A.; Vidal-Madejar, C.; Guiochon, G. HRC&CC 1985, 8, 591.

3. Grob, K., Jr.; Neukom, H.P. HRC&CC 1979, 2, 563.

4. Grob, K., Jr. J. Chromatogr. 1981, 213, 3.

5. Grob, K., Jr. J. Chromatogr. 1982, 237, 15.

6. Grob, K., Jr.; Schilling, B. J. Chromatogr. 1983, 259, 37.

7. Grob, K., Jr.; Schilling, B. J. Chromatogr. 1983, 260, 265.

8. Grob, K., Jr.; Schilling, B. J. Chromatogr. 1983, 264, 7.

9. Grob, K., Jr. J. Chromatogr. 1983, 279, 225.

10. Miller, R. J.; Jennings, W. HRC&CC 1979, 2, 72.

11. Fuller, E. N.; Ensley, K.; Giddings, J.C. Ind. Eng. Chem. 1966, 58, 18.

12. Fritz, J. S.; Scott, D. M. J. Chromatogr. 1983, 271, 193.

13. Nilsson, O. HRC&CC 1982, 5, 38.

14. Nilsson, O. HRC&CC 1982, 5, 143.

15. Nilsson, O. HRC&CC 1982, 5, 311.

16. Ceulemans, J. J. Chromatogr. Sci. 1984, 22, 296.

17. Ogan, K.; Scott, R. P. W. HRC&CC 1984, 7, 382.

18. Schutjes, C. P. M.; Leclerca, P. A.; Rijks, J. A.; Cramers, C. A.; Vidal-Madjar, C.; Guiochon, G. J. Chromatogr. 1984, 289, 163.

19. Nilsson, O. HRC&CC 1979, 2, 191.

20. Nilsson, O. HRC&CC 1979, 2, 605.

21. Said, A.S. HRC&CC 1989, 2, 637.

SECTION II. MEASUREMENT OF COLUMN DEAD TIME IN CAPILLARY GAS CHROMATOGRAPHY

INTRODUCTION

The accurate measurement of dead time (t_M) in gas chromatography is often necessary. For example, the measurement of Kovats indices requires accurate measurement of adjusted retention times (t_R-t_M) both of n-alkanes and of the sample compounds. The calculation of capacity factors (k′) for studies of peak broadening and for other purposes also necessitates an accurate value for t_M, since $k' = \frac{t_R - t_M}{t_M}$. Good values for t_M are especially important when the adjusted retention times (t'_R) or values of k′ are quite low.

Wainwright and Haken have published a detailed and critical review of the extensive literature on the accurate measurement of t_M in gas chromatography [1]. Other investigators have proposed both iterative and statistical methods to determine t_M mathematically [2-7]. Several of the publications reviewed show that the commonly used retention time for the methane peak usually does not give accurate values for t_M. This is because the k′ for methane under most conditions is greater than zero. Wainwright and Haken [1] also concluded that methods in which linear plots of t_M vs. carbon number for alkanes are

extrapolated to a carbon number of zero are suspect. Wainwright, Haken and Srisukh [3] have shown that such a plot is not linear for C_1-C_4 alkanes. Parcher and Johnson [5] used an extrapolation method in which methane was assigned an effective carbon number of 0.5.

The best methods for accurate calculation of t_M appear to be those in which retention times are measured for a series of n-alkanes and the best value for t_M is obtained by an iterative procedure that is based on the linearity of $\log(t_R-t_M)$ plotted against carbon number. Many of these methods require alkanes of consecutive carbon numbers [8], but some do not. Many of the procedures are surprisingly complicated [9-10].

A method is now described for measuring t_M in gas chromatography that is both simple and accurate. A sample containing several liquid n-alkanes is injected into a capillary-column gas chromatograph and the unadjusted retention times are measured. A simple iterative procedure that involves linear regression is then used to find the value of t_M that gives the best linear fit of the values of $\log(t_R-t_M)$ plotted against the carbon number of the n-alkanes. The iterative process is allowed to proceed until the value obtained for t_M is constant. Alternatively, values of log k′ can be plotted against

carbon number in order to determine the correct value of t_M. One iterative procedure can easily be carried out on a programmable hand calculator. The second iterative procedure was developed by Dr. Dan Scott and can be easily performed on a personal computer.

EXPERIMENTAL

A Hewlet-Packard 5580A gas chromatograph in the split injection mode was used with a flame ionization detector. A 12.25 m X 0.20 mm DB-1, cross-linked, methyl-silicone, capillary column was used with a film thickness of 0.33 μm. Helium was used as the carrier gas and the inlet pressure was maintained at 15.0 psi above atmospheric pressure for all chromatographic runs unless otherwise noted. Injections of 1.0 μl were made manually. The injector port was maintained at 250^{o} C and all chromatograms were run isothermally at various temperatures from 80^{o} C to 180^{o} C. The split ratio was 320:1 for the temperature study, and a range of 39:1 to 435:1 was used in the split ratio study.

The C_7-C_{12} n-alkanes were quantitative grade from Polyscience Inc. and the pentane solvent was glass distilled. Samples were prepared by adding 1.0 μl of each n-alkane to 1.0 ml of pentane. Kovats indices were calculated on reagent grade samples.

Retention times were given by the Hewlett-Packard 5880-A integrator to the nearest 0.001 min. Each sample was chromatographed a minimum of three times and the average retention time was used in all calculations.

Typically, the retention times were identical for all three runs, with any variation in retention time being less than a 0.2% relative standard deviation.

RESULTS AND DISCUSSION

A plot of log k′ versus carbon number is very linear for the liquid n-alkanes (C_5 and above). However, if an incorrect t_M (such as $t_M = t_R$ for methane) is used to calculate the k′ values, the plot will depart from linearity, especially at low k′ values. The purpose of an iterative procedure is to make the plot of log k′ versus carbon number as linear as possible.

METHOD I

The retention times of several n-alkanes are measured under fixed conditions (carrier gas inlet pressure, column temperature, split ratio, etc.) and the average of 3 or 4 runs is taken. A provisional value is taken for t_M that is a little less than the t_R for the lowest alkane. This value of t_M is used to calculate the various k′ values (or adjusted retention times, t_R-t_M) and a linear regression is performed for log k′ (or log (t_R-t_M) against carbon number, C. The regression is used to calculate a new value for the k′ value (or (t_R-t_M) value) for the lowest alkane (usually C_5 or C_7), and thus obtain a new value for t_M. The new t_M is used to recalculate new values for the k′ values and a regression is used to find a new value for the lowest alkane. After several such iterations a value

Figure 1. Flow chart of computer program to determine t_M using a Hewlett Packard 11-C calculator

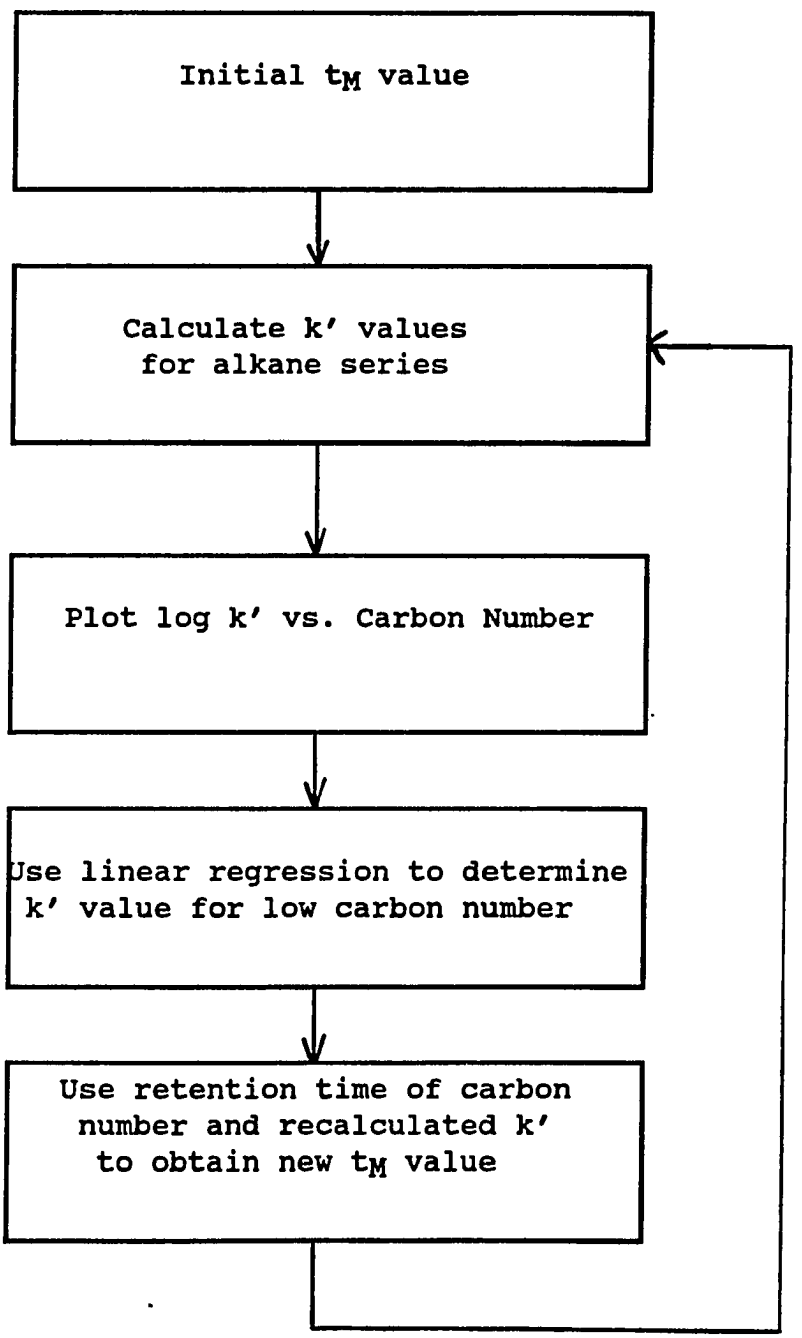
Initial t_M value
Calculate k' values for alkane series
Plot log k' vs. Carbon Number
Use linear regression to determine k' value for low carbon number
Use retention time of carbon number and recalculated k' to obtain new t_M value

is found for t_M that does not change. Figure 1 illustrates the flow diagram for this program.

Figure 2 shows that when the retention time of methane is used for the t_M value, the plot of log k' versus C is not linear for low values of C. However, after several iterations, this relationship quickly approaches a linear function.

The final value of t_M is used to calculate values of k' (or t_R-t_M), which should give an excellent correlation coefficient (0.99999 or better) for the plot of log k' versus C. Some results are given in Table I. A program for the iterative calculation using a popular calculator is given in Appendix I. This program uses 25 iterations, which is probably excessive. However, this assures a constant value for t_M, regardless of the initial value chosen for t_M.

Virtually any reasonable initial value of t_M converges to the same final t_M value. Table II shows the value of t_M obtained from different initial estimates. As can be seen, the function converges to the correct value of t_M. This eliminates the need for making a methane injection, since any initial estimate slightly less than the retention time of the earliest eluting peak will converge to the correct value of t_M.

Figure 2. Plot of log k′ vs. n-alkane carbon number (C) using different values for t_M obtained from computer program. Solid line: retention time of methane used for t_M. Dashed line: t_M value obtained after five iterations. Dotted line: t_M value obtained after ten iterations

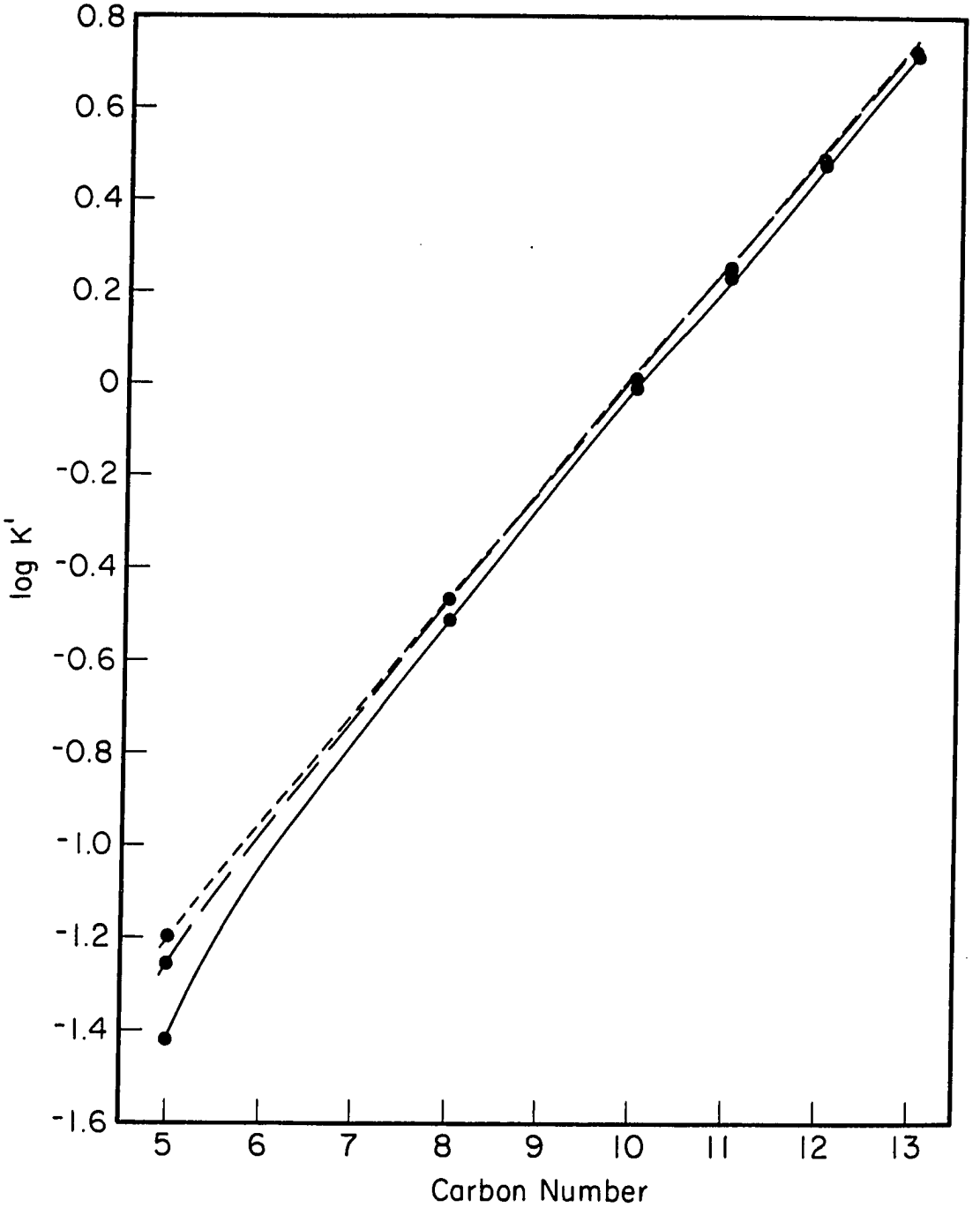
0.8
0.6
0.4
0.2
0
-0.2
-0.4
-0.6
-0.8
-1.0
-1.2
-1.4
-1.6
log K'
5
6
7
8
9
10
11
12
13
Carbon Number

Table I. Comparison of Methods I and II for linear regression of log k′ = mC + b. C = Alkane Carbon Number. P_i = 15 psi

	Method I			Method II		
T °C	$t_M$sec	m	b	$t_M$sec	m	b
80	29.52	0.3089	-2.388	29.48	0.3087	-2.384
100	30.90	0.2754	-2.391	30.88	0.2753	-2.290
120	32.22	0.2468	-2.397	32.20	0.2465	-2.393
130	32.70	0.2319	-2.373	32.73	0.2322	-2.377
140	33.18	0.2201	-2.381	33.18	0.2200	-2.379
150	33.90	0.2085	-2.378	33.88	0.2082	-2.375
160	34.32	0.1970	-2.369	34.36	0.1972	-2.372
180	35.58	0.1805	-2.408	35.47	0.1785	-2.383

Table II. Determination of t_M using different values for the initial estimate of t_M. Retention time of methane is 40.26 sec; the retention time of pentane is 42.06 sec. Temperature = 120 °C. P_i = 12 psi

Initial Estimate (sec)	t_M Value (sec)	y[a]	m[b]	r[c]
37.86	39.73	-2.397	0.2468	0.999999
38.40	39.73	-2.398	0.2469	0.999999
39.78	39.76	-2.401	0.2472	0.999999
40.08	39.77	-2.401	0.2472	0.999999
40.26	39.77	-2.402	0.2473	0.999999
40.80	39.77	-2.401	0.2472	0.999999
42.06	39.80	-2.406	0.2476	0.999998

[a]y-intercept.
[b]Slope.
[c]Correlation coefficient.

METHOD II

Values of t_R for several alkanes are measured as in Method I. In this method we seek to find that value of t_M for which the regression of $y = \log(t_R - t_M)$ against x = carbon number has the smallest possible sum of squared error (SSE). Minimizing the SSE is of course the classical method for finding the best straight-line fit to a set of data.

The sum of squared error depends on the value of t_M used in the calculation of the y values. The value of t_M that yields the smallest value for SSE could be found by trial and error, but this would be needlessly time consuming. Instead a computer program for finding the best value for t_M was written using MATLAB, a matrix manipulation program which is in the public domain. The point at which SSE is a minimum is where its derivative with respect to t_M is zero. We used Newton's method to find this point. Twenty iterations of Newton's method were used, which is probably much more than necessary. A complete listing of the MATLAB program is given in Appendix II.

The programmed iterations converged quickly to the same t_M value when any of several initial values of t_M were taken that were a little lower than the t_R for the

lowest alkane. However, when lower estimates for initial t_M are taken, a considerably lower final value for t_M will generally be obtained. This happens either because the SSE has a maximum as well as a minimum or because the SSE (t_M) function becomes nearly flat without having a minimum or a maximum. After the program has been run, the value of the second derivative can be called up by pressing der2 and the return key. A positive sign indicates a minimum for SSE and a correct value for t_M. A negative sign indicates a maximum for SSE and that a higher initial estimate for t_M is needed.

This program for calculating t_M is short and easy to run. It is computationally more efficient than programs, such as that of Guardino et al. [11], that have been used previously. Almost any estimate for the initial t_M that is not too far below the lowest data point will converge rapidly to the same final t_M value.

The t_M values for several runs at varying temperatures calculated by Method I and Method II are given in Table I. It is a common practice to compare a new method of determining t_M with existing methods [12-15]. Using recently published data for several types of capillary chromatographic columns [16], t_M values calculated by both methods are given in Table III. These t_M values are also

Table III. Comparison of t_M values calculated by published methods and by the methods proposed here using data from reference 11, Tables I and II

Column	t_M (sec) (Ave. of 3 methods)	Range (sec)	t_M (sec) Method I	t_M (sec) Method II
OV-101	30.36	0.44	31.24	30.47
OV-3	30.03	0.62	30.00	29.86
OV-7	31.50	0.48	32.24	31.16
OV-11	31.67	1.03	31.45	31.58
OV-17	31.12	0.72	31.26	30.96
OV-22	28.29	1.05	28.32	28.27
OV-25	30.75	0.51	30.44	30.66

compared with the average of three other methods [16]. In general the values of t_M calculated by Methods I and II are in excellent agreement. However, the method of calculation in the first method places considerable stress on the accurate measurement of t_R for the lowest alkane used. Method II places more equal weighting on all of the data points and therefore should be slightly more accurate.

Effect of Temperature

It is known qualitatively that at a fixed inlet pressure the value of t_M tends to increase with increased column temperatures. This is because higher temperatures cause more rapid movement of carrier gas molecules, resulting in a higher back pressure. The data in Table I show that t_M increases in essentially linear fashion with increased temperature.

Figure 3 shows the effect of increasing temperature on t_M, and the retention times of methane, pentane, octane, and nonane. It is interesting that not only does the retention time of methane increase in a parallel manner to t_M, but that the retention times of the other alkanes also increase after a temperature characteristic for each alkane is reached. This shows that a limit exists for

Figure 3. Plot of retention times of nonane (C_9), octane (C_8), pentane (C_5), methane (CH_4) and t_M as a function of temperature. Split ratio: 320:1. Inlet pressure: 15.0 psi above atmospheric pressure

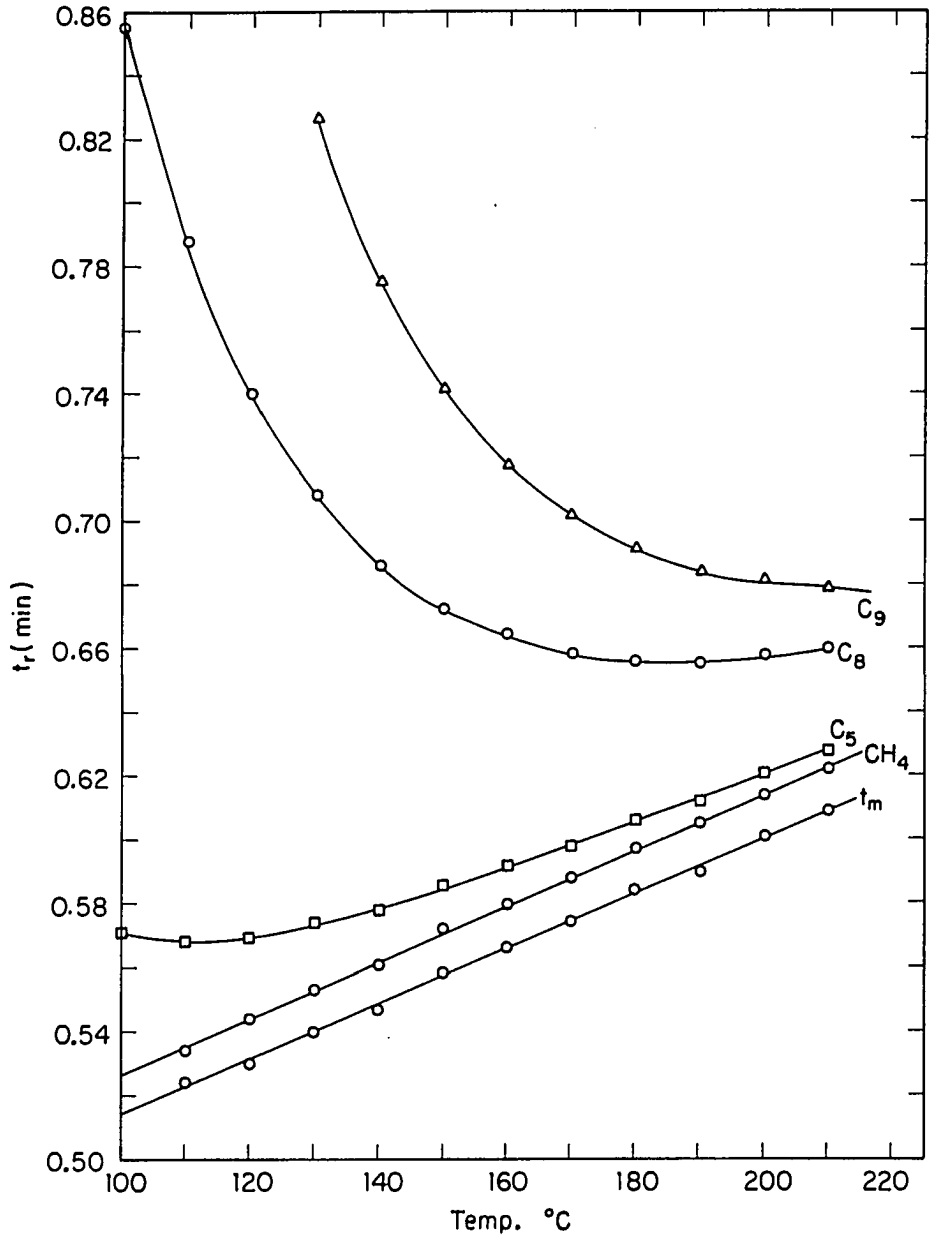
0.86
0.82
0.78
0.74
0.70
0.66
0.62
0.58
0.54
0.50
t_r (min)
100
120
140
160
180
200
220
Temp. °C
C_9
C_8
C_5
CH_4
t_m

reducing an analyte's retention time by simply increasing the column temperature.

The slopes of the plot of log k' versus carbon number are also given in Table I. These decrease in linear fashion when plotted against the log of temperature (correlation coefficient = -0.9995). The reason for this is that a plot of log k' against log temperature is linear for each of the alkanes, but the slope of these plots increases with increasing carbon number. Therefore, the difference in log k' between alkanes of different carbon number becomes less at higher temperatures.

Effect of Split Ratio

Numerous measurements of t_M were made keeping the temperature and carrier gas inlet pressure constant, but changing the split ratio. The data obtained both for t_M and for the retention time of methane are plotted in Figure 4. There is some scatter of points at the lower split ratios, possibly owing to some inconsistencies resulting from manual sample injection and from changes in atmospheric pressure (see below). Nevertheless, the t_M values and t_R values for methane show a definite decrease as the split ratio becomes larger. The difference between t_R for methane and t_M is essentially the same at all split ratios.

Figure 4. Plot of retention time of methane and t_M as a function of split ratio. Column temperature: 150° C. Inlet pressure: 15.0 psi above atmospheric pressure

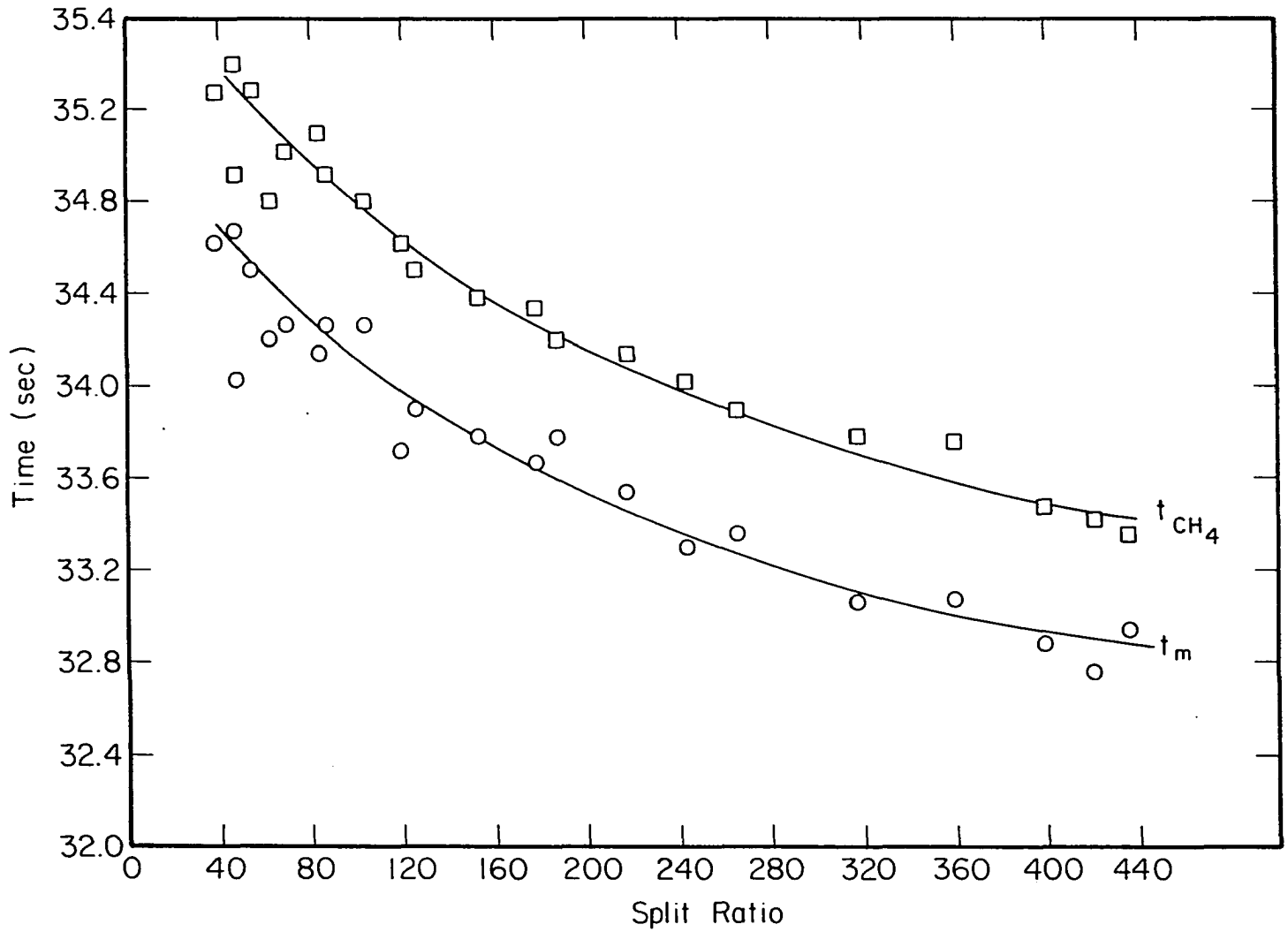
35.4
35.2
34.8
34.4
34.0
33.6
33.2
32.8
32.4
32.0
Time (sec)
0
40
80
120
160
200
240
280
320
360
400
440
Split Ratio
t_{CH_4}
t_m

Effect of Pressure

The carrier gas flow rate and hence the value of t_M is a linear function of pressure, $p_i - p_o$, where the subscripts i and o refer to the column inlet and outlet, respectively. At a fixed setting of p_i the value of t_M will fluctuate from day to day because of changes in atmospheric pressure that affect p_o. It is therefore a good idea to check the value of t_M daily.

Kovats Retention Indices

The determination of Kovats indices (I) is related to the adjusted retention times of normal alkanes according to the following equation:

$$\log (t_C - t_M) = mZ + b$$

where t_C is the retention time of a n-alkane of carbon number C, T_M is the column dead time and Z = 100C for the n-alkanes. By measuring t_C for a series of n-alkanes and calculating t_M by one of the methods described above, the constants m and b can be evaluated. The Kovats index (I) for any compound (X) can then be calculated from the retention time (t_X), determined under exactly the same conditions used for the n-alkanes.

$$\log (t_X - t_M) = mI + b$$

This method for calculating Kovats indices is more convenient than the classical method which requires that each sample compound to be measured be bracketed by n-alkanes. Measurements of several compounds showed reasonably good agreement between the two methods (see Table IV).

Calculation of k'

The correct value of k' is necessary in band broadening investigations, which requires a correct value for t_M. Table IV shows that for low k' values, a substantial error is introduced when the retention time of methane is used as t_M. The error, however, quickly diminishes as k' increases. This is also evident in Figure 2 by the linearity of the plot of log k' versus C for the larger n-alkanes, even when methane is used as t_M.

Table IV. Comparison of Kovats indices using classical method (I_a) and linear regression method I (I_b). t_M = 32.22 sec, m = 0.2477, b = -2.407

Compound	t_R sec	I_a	I_b	ΔI
Anisole	54.60	907.67	907.95	0.28
Hexanoic acid	61.26	953.25	953.52	0.27
p-Cymene	75.54	1023.44	1023.66	0.22
1-Chlorooctane	83.70	1053.77	1054.41	0.33
1-Nonanol	89.70	1073.00	1073.07	0.07
2-Nonanone	123.8	1155.34	1155.03	-0.31

Table V. Error in using the retention time of CH_4 to calculate k′ at 120°C. t_M = 32.22 sec

Carbon Number	t_r(sec)	k′ (CH_4)	k′ (t_M)	Δk′	% Error
1	32.64	------	0.0130	0.013	100.0
5	34.02	0.0423	0.0559	0.014	24.3
7	39.12	0.198	0.214	0.016	7.5
8	44.40	0.360	0.378	0.018	4.8
9	53.70	0.645	0.667	0.022	3.3
10	70.20	1.151	1.179	0.028	2.4
11	99.30	2.042	2.082	0.040	1.9
12	150.2	3.603	3.663	0.060	1.6

CONCLUSION

A mathematical method is described to determine the correct dead time of a capillary column in gas chromatography using a flame ionization detector. Based on an iterative process, the method is shown to be simple, rapid and accurate.

It is demonstrated that the retention time of methane is an incorrect value for t_M. While parameters such as temperature, pressure, and split ratio effect both t_M and the retention time of methane in a similar fashion, there is a significant difference in the two values. Thus, the use of the retention time of methane to calculate capacity factors or Kovats indices will be incorrect, especially for early eluting peaks.

REFERENCES

1. Wainwright, W. S.; Haken, J. K. J. Chromatogr. 1980, 184, 1.

2. Sevcik, J.; Lowenstap, M. S. H. J. Chromatogr. 1978, 147, 75.

3. Wainwright, W. S.; Haken; J. K.; Srisukh, D. J. Chromatogr. 1980, 188, 246.

4. Ettre, L. S. Chromatographia 1980, 13, 73.

5. Parcher, J. F.; Johnson, D. M. J. Chromatogr. Sci. 1980, 18, 267.

6. Toth, A.; Zola, E. J. Chromatogr. 1984, 284, 53.

7. Toth, A.; Zola, E. J. Chromatogr. 1984, 298, 381.

8. Hansen, H. L.; Andresen, K. J. Chromatogr. 1968, 34, 246.

9. AL-Thamir, W. K.; Purnell, J. H.; Wellington, C. A.; Laub, R. J. J. Chromatogr. 1979, 173, 388.

10. Grobler, A.; BÁLais, G. J. Chromatogr. Sci. 1974, 12, 57.

11. Guardino, X.; Albaiges, J.; Firpo, G.; Rodriguez-Vinals, R.; Gassiot, M. J. Chromatogr. 1976, 118, 13.

12. Smith, R. J.; Haken, J. K.; Wainwright, M. S. J. Chromatogr. 1978, 147, 65.

13. García Domínquez, J. A.; Munoz, J. G.; Sánchez, E. F.; Molera, M. J. J. Chromatogr. Sci. 1977, 15, 520.

14. Budahegyi, M. V.; Lombosi, E. R.; Lombosi, T. S.; Meszaro, S. Y.; Nyiredy, S.; Tarján, G. T.; Takács, J. M. J. Chromatogr. 1983, 271, 213.

15. Touabet, A.; Badjahmadj Ahmed, A. Y.; Maeck, M.; Meklat, B. Y. HRC&CC, 1986, 9, 456.

APPENDIX I

Program for calculating t_M on programmable Hewlett-Packard calculators.

```
f LBL A                                  10^X
01.02501                                  1
STO I                                     +
f LBL 1                                  1/X
RCL I                                    RCL .1
g INT                                    X
f PSE                                    STO .0
f CLEAR Σ+                               f PSE
RCL .1                                   f ISG
GSB 0                                    GTO 1
(first C of series)                      g RTN
Σ+                                       f LBL 0
RCL .2                                   RCL .0
GSB 0                                    +
(second C of series)                     1
Σ+                                       -
  .
( . Repeat proceeding four steps
  .
    for each member of series)           g LOG
  .
  .
  .
(last C of series)                       g RTN
Σ+                                       g P/R
(first C of series)
  ^
f Y
```

The retention time of each alkane in the series is stored in a different register, with the first provisional value of t_M always stored in register .0. The corresponding carbon number (C) is then written into the program. For example, in our study, the retention times for the n-alkane series of heptane through dodecane were entered into registers .1, .2, .3, .4, .5, and .6, respectively. Obviously, the first C of the series is 7; the second, 8; and the last, 12. This program is easy to modify for different sets of alkanes. Since log k' is used, units for retention time can be either in minutes or seconds.

APPENDIX II

In this appendix we give a listing of the MATLAB program which was used in estimating t_M by method II. The program was run on a Zenith Z148 personal computer with 512k ram. (An IBM PC compatible). Before the program is run MATLAB must be loaded and an initial guess for t_M (t_M) must be chosen. Note that x is a column vector containing the carbon numbers of the n-alkanes, while ret is another column vector containing the experimentally measured retention times of the n-alkanes. After the program is run the value of t_M will be the corrected value for the dead time, while the vector mb will contain the slope and intercept of the regression line.

```
en=ones(x);
rmat=<x,en>;
Q=eye-(rmat*inv(rmat'*rmat)*rmat');
for i= 1:20, cret = ret-tm*en, ...
y = log(cret), yp=-en./cret, ypp = -yp.*yp, ...
der2=((yp'*Q*yp)+(y'*Q*ypp)), ...
tm=tm-((y'*Q*yp)/der2);
y=log((ret-tm*en)/tm)/log(10);
mb=inv(rmat'*rmat)*rmat'*y;
```

SECTION III. INJECTION PEAKS IN ANION CHROMATOGRAPHY

INTRODUCTION

In single-column, ion chromatography (SCIC) the first peak is always the injection peak, which is caused by the displacement of eluent ions by the injected sample. It may be either positive or negative, depending on the concentration of the injected sample to which this peak has been shown to be quantitatively related [1]. This has, however, never been fully interpreted, and many chromatograms shown in the literature [2,3] do not make use of the first few minutes of the chromatographic separation, although the injection peak, which occurs in that period, is a potentially rich source of information.

Several investigators have dealt with the appearance of chromatographic peaks other than sample peaks, namely injection and system peaks. They have pointed out that these are due to the fact that the eluent contains more than one component. Stranahan and Deming [4] explained them as being caused by the change that occurs in the distribution of mobile phase components following sample injection. Levin and Grushka [5] have dealt with system peaks occurring in the chromatographic separation of amino acids when using acetate buffers as eluents. Hummel and Dreyer [6] have applied gel permeation chromatography to

the investigation of protein binding to small molecules. They showed that the appearance of an injection and a system peak is the result of injecting a protein sample and a ligand onto a column pre-equilibrated with that ligand and in the same concentration.

Two effects contribute to the area of the injection peak. The first is the displacement of eluent ions, caused by the adsorption of the sample ions on the ion-exchange column. The second is the dilution of the eluent ions which occurs when the sample is more dilute than the eluent. The first effect tends to increase the area of the injection peak. The second effect tends to reduce the area of the injection peak, which is why negative injection peaks are observed in many chromatograms cited in the literature [3].

The second effect can be overcome by preparing the sample so that it has the same concentration of eluent ions as that of the mobile phase. The result is a positive injection peak which can be related to the concentration of the sample.

The aim of this work was to show that the injection peak area of a salt in anion chromatography is proportional to the cationic content of that salt. By combining the information obtained from the injection peak

and from the sample peak, mixtures of salts in acidic, alkaline or neutral solutions can be quantitated.

EXPERIMENTAL

The chromatographic system was built from several components. An LKB 2150 High-Performance Liquid Chromatography (HPLC) pump was used to control eluent delivery. A Wescan ICM II ion analyzer with conductivity detection was maintained at a constant temperature. Samples were introduced through a Rheodyne Model 7125 injection valve fitted with a 100 μl loop. A Shimadzu CR3A integrator was used in conjunction with a Curkin Scientific strip chart recorder. The peak retention times, areas and heights were obtained from the integrator. All separations were effected with a commercial Wescan 269-029 anion-exchange column (25 cm). the flow-rate of the eluent, 1.5×10^{-3} M sodium phthalate (pH 4.3), was maintained at 1.0 ml/min.

Standard solutions were prepared with reagent-grade chemicals and with deionized water (Milli Q Reagent Grade Water System). The concentration of the salt solutions injected ranged from 0.2×10^{-3} to 1.0×10^{-3} M. All solutions were prepared in 1.5×10^{-3} M sodium phthalate (pH 4.3) by the addition of 10.00 ml 1.5×10^{-2} M sodium phthalate before diluting the sample to 100 ml. The injection of each solution was repeated three times, and

the average value was used, the relative standard deviation being lower than 2%.

RESULTS AND DISCUSSION

Injection Peak

The size of the injection peak of a salt solution containing the same concentration of the eluent as the mobile phase depends mainly on the cation content of that salt. This is illustrated in Figure 1, which shows injection peak areas of various sodium salt versus concentration. The linear correlation between the sodium concentration and the peak area is independent of the salt's anion: all points for three different sodium salts fall on one and the same straight line passing through the origin at zero salt concentration. This can be explained as follows: If a sodium salt solution is injected into a chromatographic anion-exchange column, the anion of the salt is retained on the column, displacing eluent ions. In the present case the eluent is sodium biphthalate (buffered at pH 4.30), and biphthalate ions will accordingly be displaced, the injection peak area being proportional to

$$pA \propto \lambda_{Na^+}[Na^+] + \lambda_{HP^-}[HP^-] + 2\lambda_{P^{2-}}[P^{2-}] \qquad (1)$$

where pA = peak area in arbitrary units; λ_n = the equivalent conductivity of the conducting species, n, in

Figure 1. Injection peak areas of various sodium salts as a function of concentration: □ = NaCl; O = NaOH; Δ = NaO_2CCH_3

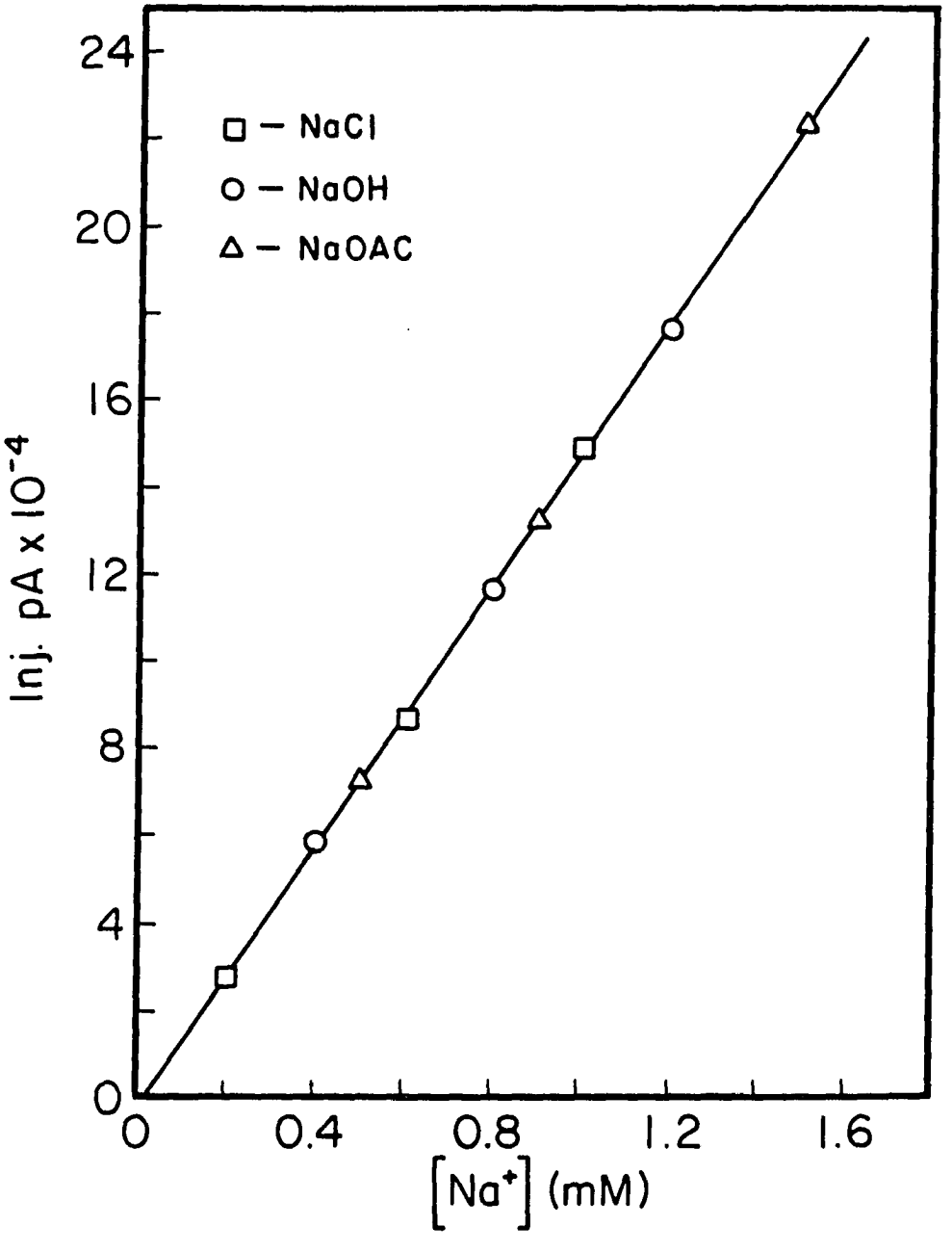
□ – NaCl
○ – NaOH
△ – NaOAC
Inj. pA x 10⁻⁴
24
20
16
12
8
4
0
0
0.4
0.8
1.2
1.6
[Na⁺] (mM)

aqueous solution; and HP^-, P^{2-} = biphthalate and phthalate anions.

The area of the injection peak is therefore dependent on the cation content of the sample and on the composition of the eluent before and after injection. It is thus dependent only on the concentration of the anion injected and independent of its type.

Quantitative Relationship Between Injection and Sample Peaks

The quantitative relationship between the areas of the injection peak and of the sample peak can best be illustrated by the data in Table I, which shows that there is a certain ratio between the areas of the injection peak and of the sample peak. The ratios listed in Table I are characteristic of the injection of sodium chloride solutions.

The two peaks obtained by injecting only one salt have different meanings.

The response of the detector comprising the injection peak area (in arbitrary units) measures the difference between the conductivity of the displaced eluent ions plus that of the sample's cation, and the "background conductivity" of the eluent. This can be represented mathematically as follows:

Table I. Injection and sample peak areas of sodium chloride solutions. Eluent: 1.5×10^{-3} M NaHP at a pH value of 4.30

Concentration of NaCl (mM)	Injection Peak Area	Cl^- Peak Area	Peak Area Ratio
0.2	33820 (1.0% RSD)	16702 (1.2% RSD)	2.025
0.4	64544 (0.70%)	34731 (0.57%)	1.858
0.6	94254 (0.71%)	53410 (0.7%)	1.764
0.8	124855 (0.41%)	72215 (0.12%)	1.729
1.0	154971 (0.62%)	90625 (0.08%)	1.710

$$10^{-3} K\Delta G_{inj} = \lambda_{Na^+}[Na^+]_2 + \lambda_{HP^-}[HP^-]_2 + 2\lambda_{p2-}[P^{2-}] - B \quad (2)$$

where the term $B = \lambda_{Na^+}[Na^+]_1 + \lambda_{HP^-}[HP^-]_1 + 2\lambda_{p2-}[P^{2-}]_1$ is the background conductivity, and $\lambda_{Na^+} = 50$, $\lambda_{HP^-} = 38.2$, and $\lambda_{p2-} = 76.4$ cm^2 equiv.$^{-1}$ Ω^{-1}, K = conductivity cell constant and $\Delta G_{inj.}$ = detector response to injection.

From equation 2, it is easy to see why the injection peak in single-column anion exchange chromatography can be either positive or negative. If the concentration and equivalent conductance of the sample's cations, and displaced eluent anions, is greater than the background conductance, B, a positive injection peak will be produced. If the concentration and equivalent conductance of the sample's cations is less than background conductance, then a negative injection peak is produced. However, when the same concentration and pH value of eluent ions, as are present in the mobile phase, is added to the sample, the "B" term in equation 2 is cancelled. The result is always a positive injection peak for an injected sample.

The sample peak, for its part, measures the difference between the conductivities of the sample and of the background, respectively. This can be expressed as

$$10^{-3} K\Delta G_s = (\lambda_{Na^+} + \lambda_{Cl^-}) I_s C_s - B \quad (3)$$

where G_S = sample peak conductivity, λ_{Cl^-} = 76.3 cm^2 $equiv.^{-1}$ Ω^{-1}, C_S = concentration of the sample and I_S = fractional ionization of the sample (which equals unity in the present case).

Dividing equation 2 by equation 3 gives the ratio of the peak areas as compiled in Table I for the specific case in which the eluent is sodium phthalate at a pH value of 4.30. The injection peak areas of salts other than of sodium can be calculated in the same manner, taking into account the appropriate equivalent conductivity data.

The numerical value of the injection peak conductance, calculated from equation 2, for 2 x 10^{-4} M NaCl is 0.0182, and for the sample peak is 0.00926. The ratio between the two conductances is 1.965, which is in good agreement with the experimental value given in Table I (2.025). As can be seen from Table I, the ratio decreases somewhat as the concentration of the injected sample is increased. This can be explained by the redistribution of phthalate species with increasing concentration of the injected sample.

Binary Salt Mixtures

Data obtained from the injection peak and the sample peak permit the quantitation of cations in binary salt

Figure 2. Injection peaks and sample peaks of three different chloride salts

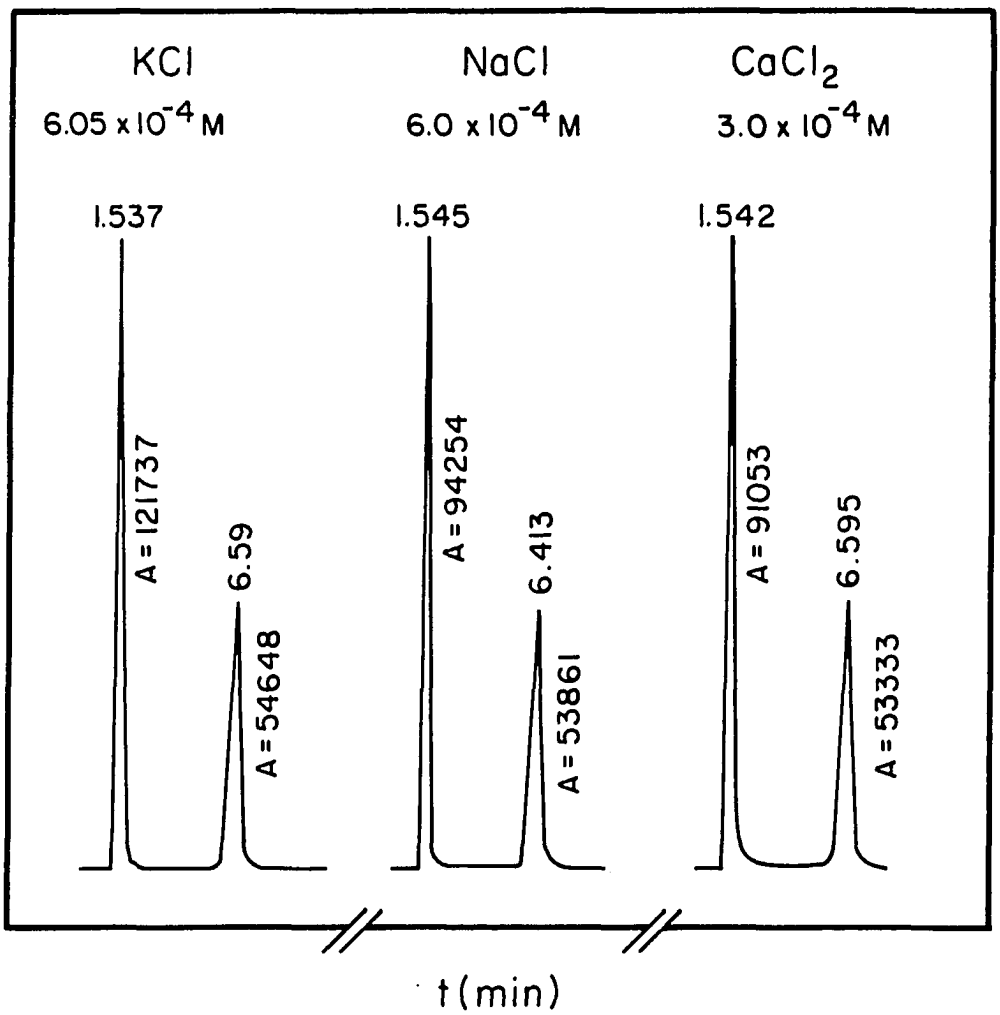
KCl
6.05 x 10⁻⁴ M
1.537
A = 121737
6.59
A = 54648
NaCl
6.0 x 10⁻⁴ M
1.545
A = 94254
6.413
A = 53861
CaCl₂
3.0 x 10⁻⁴ M
1.542
A = 91053
6.595
A = 53333
t (min)

mixtures. Figure 2 shows three chromatograms of the chloride salts of different cations. The chloride concentration is identical for all three salts, and their sample peaks therefore have the same areas; but the injection peaks are different. Potassium chloride, because of its high equivalent conductivity, has the largest peak area. The ratio between the injection peak areas of KCl and NaCl is 121,737/94,254 = 1.292: the calculated ratio from equations 2 and three is 1.283. It is thus equal to the ratio of the equivalent conductivities of KHP and NaHP multiplied by the ratio of their concentrations.

The case of $CaCl_2$ is somewhat different. The equivalent conductivity of Ca^{2+} is higher than that of Na^{+} (59 versus 50 cm^2 $equiv.^{-1}$ Ω^{-1}), but the peak area of Ca^{2+} is smaller than that of Na^{+}. The reason is that a divalent ion such as Ca^{2+} will partially interact with P^{2-} to form non-conducting calcium phthalate.

An important fact, however, is that for all three salts the correlation between the cation concentration and the injection peak area is linear, as shown in Figure 3. Combining the information from the injection peak and sample peak areas enables the composition of binary salt mixtures to be determined.

Figure 3. Injection peaks of salts of K^+, Na^+, and Ca^{2+} as a function of concentration

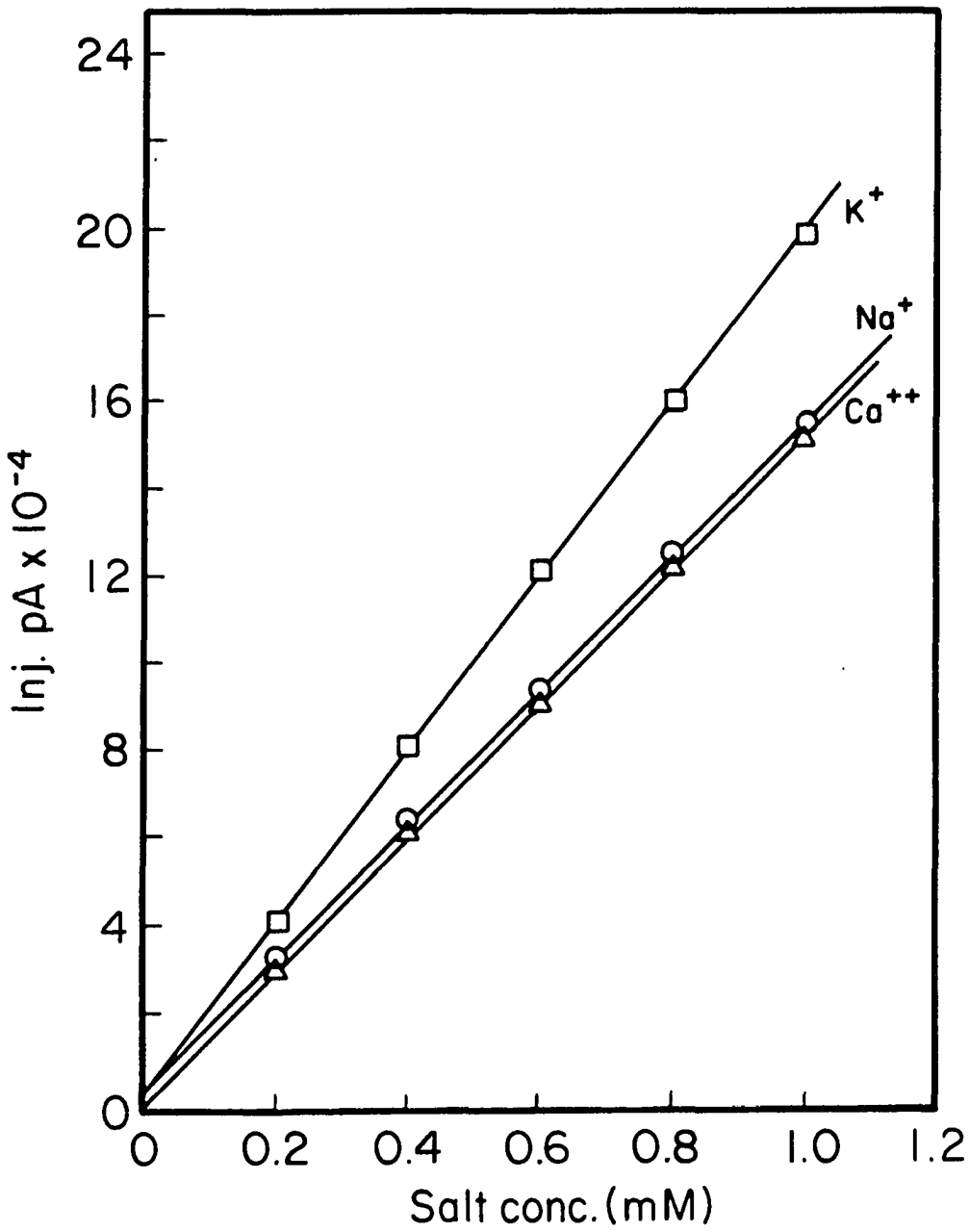
24
20
16
12
8
4
0
Inj. pA x 10⁻⁴
0
0.2
0.4
0.6
0.8
1.0
1.2
Salt conc. (mM)
K+
Na+
Ca++

For example, when a mixture of KCl and NaCl is injected the injection peak area can be expressed as

$$\text{Injection peak area} = pA_{inj.} = m[Na^+] + n[K^+] \quad (4)$$

where m and n are the respective slopes of the straight lines of the salts in Figure 3. The sample peak area can be expressed as

$$\text{Sample peak area} = pA_{Cl^-} = b([Na^+] + [K^+]) \quad (5)$$

where b is the slope of the calibration line (area versus concentration) of chloride ions in Figure 4.

There are two unknowns in equations 4 and 5, namely $[Na^+]$ and $[K^+]$. They can be accurately determined by measuring the areas of the injection peak and the sample peak and substituting the slopes of the calibration graphs.

Thus, the concentration of each constituent can be derived from equations 4 and 5:

$$[K^+] = \frac{\frac{pACl^-}{b} - pA_{inj}}{m - n}$$

$$[Na^+] = \frac{pACl^-}{b} - [K^+]$$

Figure 4. Calibration graphs of injection peaks and sample peaks needed for the quantitation of a mixture of NaCl and KNO_3

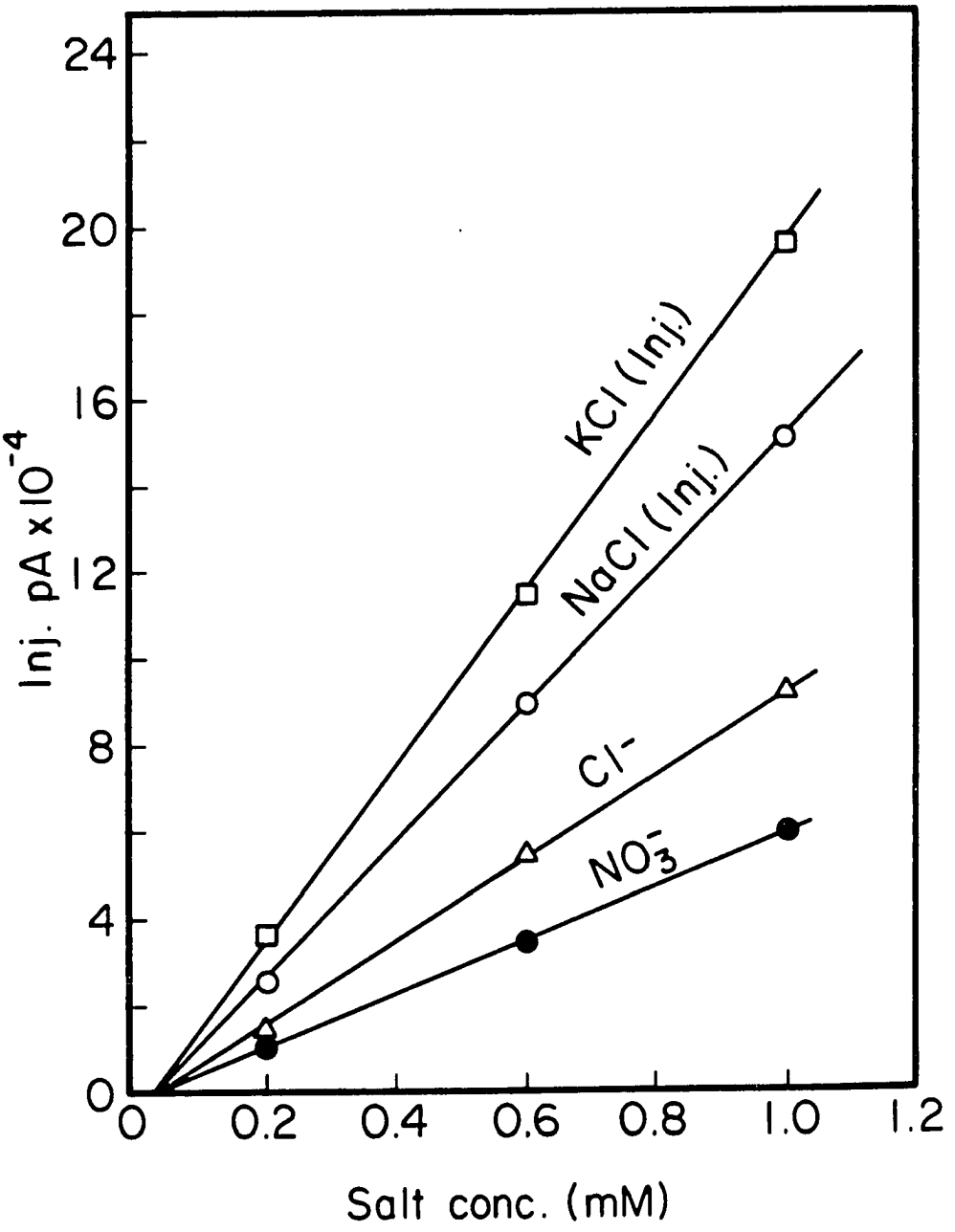
24
20
16
12
8
4
0
Inj. pA x10^{-4}
KCl (Inj.)
NaCl (Inj.)
Cl$^-$
NO$_3^-$
0
0.2
0.4
0.6
0.8
1.0
1.2
Salt conc. (mM)

In the case of two salts with two different anions, two sample peaks are available for the determination of the binary mixture. It is therefore quite possible that three salts with different anions can also be determined simultaneously.

Determination of Salt Mixtures in the Presence of an Acid or a Base

The cations of salt mixtures can be determined quantitatively in the presence of dilute acids and bases. Acidic solutions of salt mixtures can be determined quantitatively as described before. When HCl with the eluent (NaHP 1.5×10^{-3} M), but no salt is injected into the column, the injection peak areas are very small, as is seen in Figure 5. This is because the added H^+ converts some HP^- into H_2P, and the overall effect is small. If salts are injected in the presence of HCl, that effect will be even smaller, because much more HP^- is displaced and only a small part of it is converted into H_2P. The end result is that the area of the injection peak of HCl in the presence of salts is negligible. As is also seen from Figure 5, the straight line plot of the injection peak areas of NaCl and HCl samples intersects with the origin and is identical with the line for NaCl alone in Figure 1.

Figure 5. Injection peak calibration graphs for NaCl in the presence of HCl and NaOH

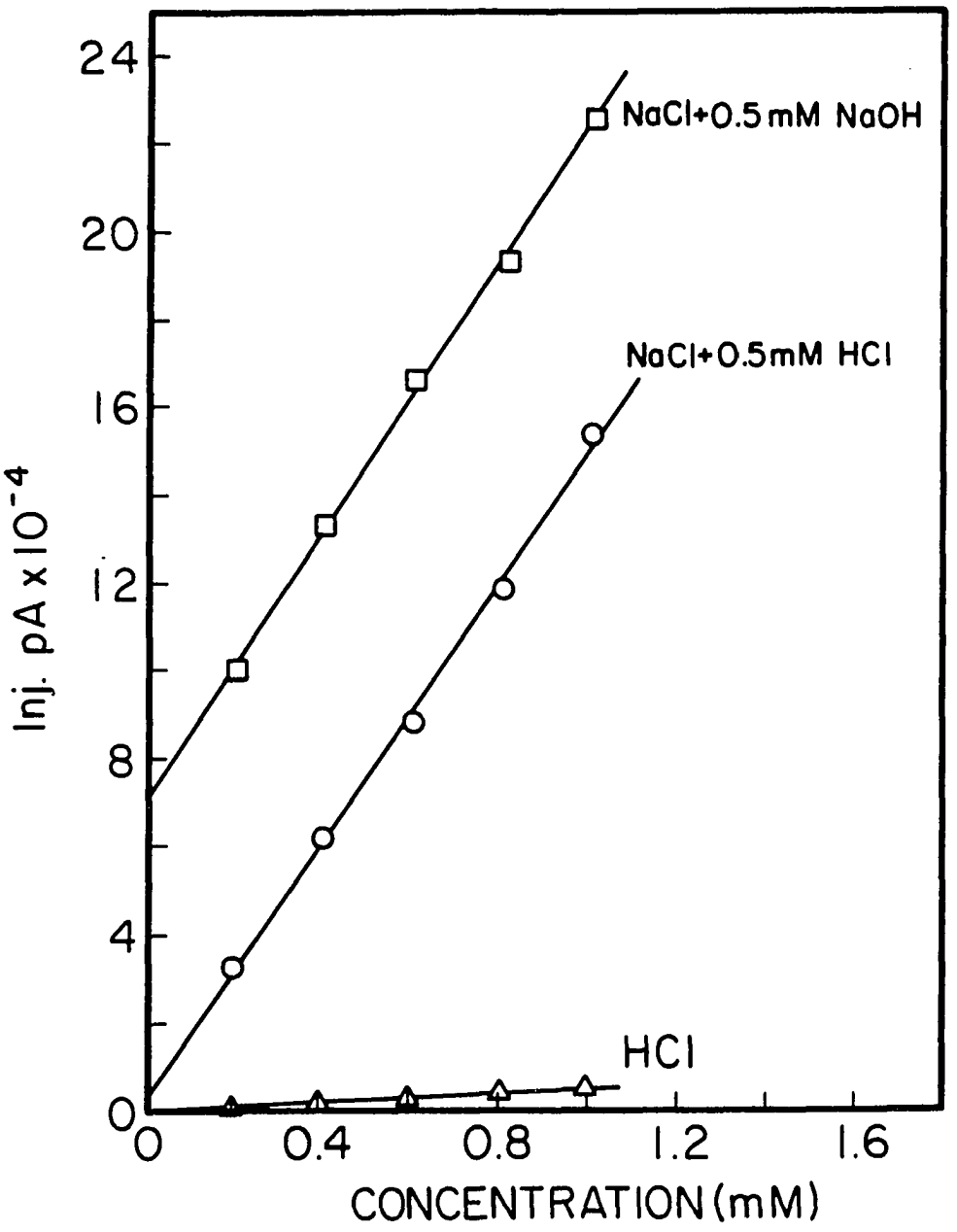
24
20
16
12
8
4
0
Inj. pA x 10⁻⁴
NaCl+0.5 mM NaOH
NaCl+0.5mM HCl
HCl
0
0.4
0.8
1.2
1.6
CONCENTRATION (mM)

In alkaline solutions, the addition of OH^- does not appreciably affect the injection peak, because some HP^- is converted into P^{2-}. However, the sodium ion from the NaOH increases the injection peak area. This is also illustrated in Figure 5, where a mixture of NaOH and NaCl yields a straight line parallel to that for NaCl and HCl; but its intercept is much higher because the added sodium ions contribute to the injection peak area. There is, of course, a limit to the acid or base content of a sample that can be tolerated.

Experimental results of the quantitation of a solution containing known concentrations of NaCl and KNO_3 are shown in Table II. Each determination was made three times, and the data for the chromatographic peaks obtained were compared with those of the calibration lines of Figure 4. From Table II, there is good correspondence between the experimental data for the mixture and the data obtained by injecting each constituent separately. The relative error of the determinations does not exceed 3%, and it is interesting that the relative standard deviations of the injection peaks are much lower than those of the sample peaks.

Table II. Quantitative Determination of a Salt Mixture in the Presence of an Acid or a Base[a]

Composition of Injected Sample	pA_{inj} of Mixture	pA_{inj} (Na^+)	pA_{inj} (K^+)	Sum	Rel. Error (%)
NaCl + KNO_3	207,485 (0.46)[b]	89,275 (0.3)	114,737 (0.03)	204,010	1.7
NaCl + KNO_3 + NaOH	301,766 (0.2)	89,275 x 2	114,737	293,290	2.89
NaCl + KNO_3 + HCl	208,366 (0.2)	89,275	114,737	204,010	2.13

[a]Concentration of each salt, acid, or base was 6×10^{-4}M.
[b]Percent Relative Standard Deviation.

Sample Peak Cl^-	pA(Cl^-) (Cal. Curve)	Rel Error (%)	Sample Peak NO_3^-	pA(NO_3^-) (Cal. Curve)	Rel Error (%)
54,468 (1.8)	54,307 (0.51)	0.30	34,338 (1.6)	34,266 (0.25)	0.21
53,910 (0.5)	54,307	0.74	35,282 (1.1)	34,266	2.96
111,080 (0.2)	54,307 x 2	2.27	34,471 (1.3)	34,266	0.59

CONCLUSIONS

In single-column, ion chromatography the commonly used eluents are salts of weak organic acids, which provide the background conductivity of the eluent. When a salt solution is injected into a chromatographic anion-exchange column, anions of the eluent are displaced from the column and the constituents of the eluent are redistributed. This change in the momentary composition of the eluent, together with the injected cation (of the sample), contributes to the conductivity of the injection peak.

By taking advantage of quantitative information on cations derived from the injection peak and for anions from the sample peaks, salt mixtures may be quantitated in acidic, neutral, or alkaline solutions using anion-exchange chromatography.

REFERENCES

1. Hershcovitz, H.; Yarnitzky, C.; Schmuckler, G. J. Chromatogr. 1982, 252, 113.

2. Bidlingmeyer, B. A.; Santasania, C. T.; Warren, F. V., Jr. Anal. Chem. 1987, 59, 1843.

3. Gjerde, D. T.; Fritz, J. S. Ion Chromatography Huthig, Heidelberg, 1987.

4. Stranahan, J. J.; Deming, S. N. Anal. Chem. 1982, 54, 1540.

5. Levin, S.; Grushka, E. Anal. Chem. 1986, 58, 1602.

6. Hummel, J. P.; Dreyer, W. J. Biochim. Biophys. Acta 1962, 63, 530.

SECTION IV. LOW CAPACITY ANION-EXCHANGE RESINS

INTRODUCTION

During the past twenty-five years, ion-exchange chromatography has undergone many improvements. One area of constant interest has been in the development of stationary-phase technology. Initially, polystyrene beads of low cross-linking were used. The particles were fairly large and irregular in shape [1,2]. More efficient columns were produced with the advent of smaller particles of uniform size [3].

Conversion of these resins into anion-exchange material suitable for chromatography is accomplished by several methods. Many commercial columns are prepared by lightly sulfonating the resin and agglomerating quaternized latex onto the surface by electrostatic forces [4]. Barron and Fritz [5] demonstrated the versatility of chloromethylating the resin and chemically attaching a quaternary ammonium functional group. A third method is to coat the resin with a quaternary ammonium monomer which contains a hydrophobic moiety such as a long-chain alkane [6-10]. These monomers are then held to the resin by hydrophobic forces. Typically, the monomer must be added to the mobile phase or eluent.

Warth et al.[11] demonstrated that small, highly functionalized, latex particles could be hydrophobically adsorbed onto non-porous, polystyrene beads to produce efficient chromatographic separations. Several parameters could be varied to change the capacity. The preparation of these resins was very simple and fast.

In an effort to coat the polystyrene beads more evenly and increase chromatographic efficiency, a latex which contains only 54% functionalization was used to coat 4.5 μm, nonporous, spherical, polystyrene beads. This resin not only has good chromatographic efficiency, but offers a unique selectivity and permits the rapid analysis of inorganic anions and biologically important dicarboxylic acids. It is also demonstrated that an organic modifier, such as methanol, can be added to the eluent to alter the selectivity of this resin.

EXPERIMENTAL

Apparatus

The chromatographic systems consist of the following components. The first system consisted of a Milton-Roy mini-pump (Laboratory Data Control, Rivera Beach, FL); A Rheodyne Model 7000 injection valve, (Ranin, Waburn, MA), equipped with a 10 μl sample loop; a Milton-roy pulse dampener (Laboratory Data Control) placed between the pump and the sample injector; a Spectroflow 783 (Kratos) variable-wavelength detector. This system was used for the indirect UV detection of the analytes. Various wavelengths were used and are noted in the text.

The second system consisted of a LKB 2150 High Performance Liquid Chromatography (HPLC) pump (Pharmacia) Wescan ICM II ion-analyzer with conductivity detector (Altech, CA) and a Rheodyne model 7125 injection valve fitted with a 10 μl sample loop.

A Shimadzu HPLC column packer (Phenomenex CA) was used to pack the column at a packing pressure ranging from 3000 to 6000 psi. The columns used were 4.6 mm i.d., glass-lined, stainless steel columns (Scientific Glass Engineering, Austin TX). Column lengths ranged from 5.0 to 15.0 cm in length and are noted in the text.

Resins

A 4.5 μm spherical, nonporous, polystyrene resin with 10% divinylbenzene (DVB) crosslinking, and 0.09 μm latex suspension 54% functionalized with quaternary ammonium groups were supplied by Rohm & Haas (Spring House, PA). The latex was coated onto the polystyrene resin under various conditions to study the coating characteristics of the latex. The anion-exchange resin was prepared by continuously stirring a slurry of latex and uncoated resin. The coated resin had an exchange capacity range of 14 to 35 μeq/g. Capacities were determined by NO_3^-/SO_4^{2-} displacement method. The coated resin was packed using the upward packing method.

Reagents and Solutions

1,3,5-benzenetricarboxylic acid (BTA) (97%, Aldrich) was purified by recrystallization from boiling, distilled, deionized water (Millipore). The precipitate was filtered by suction and washed. All other chemicals were of reagent grade or better, and were used without further purification. Distilled, deionized water was used throughout.

Eluents of phthalate and BTA were prepared by dissolving the acids in water and adjusting the pH with 0.1 M lithium hydroxide. Eluents were vacuum filtered

through a 0.2 μm membrane filter and vacuum degassed. Stock solutions of sample anions were prepared from their sodium salts. Dicarboxylic acids were prepared from the acid and deprotonated with lithium hydroxide. Stock solutions of 1000 ppm were used and samples prepared by diluting aliquots of the stock solution as necessary.

RESULTS AND DISCUSSION

Resin Preparation

Previous work involving latex that had 76% and 100% functionalization demonstrated that the capacity of the coated resin was dependent on the length time the slurry was mixed, and on the concentration of NaCl and amount of functionalized latex present in the slurry [11]. In each case, capacity increased as one or more of these three parameters increased. In the present work, using only 54% functionalized latex, it was found that the final resin capacity was independent of the concentration of NaCl or the length of time the latex and substrate were mixed together. For example, after one, two, and four hours of continuous mixing, the resin had a capacity of 27.3, 26.7, and 27.7 μeq/g, respectively. This is probably due to the more hydrophobic nature of this latex. The result is that the latex quickly reached equilibrium between the resin and the aqueous slurry.

The presence of NaCl in the aqueous slurry actually had a deleterious effect when 54% functionalized latex was used. By increasing the ionic strength of the slurry, the latex hydrophobically agglomerated. This produced unevenly coated resin and inefficient chromatographic

Figure 1. Separation of 0.2 mM Cl^-, 0.3 mM NO_2^-, and 0.2 mM Br^- on a 25 cm x 4.5 mm i.d. column with a capacity of 27 μeq/g. Eluent was 0.2 mM BTA at a pH value of 7.00 and a flow rate of 1 ml/min. Resin was prepared in 0.1 M NaCl

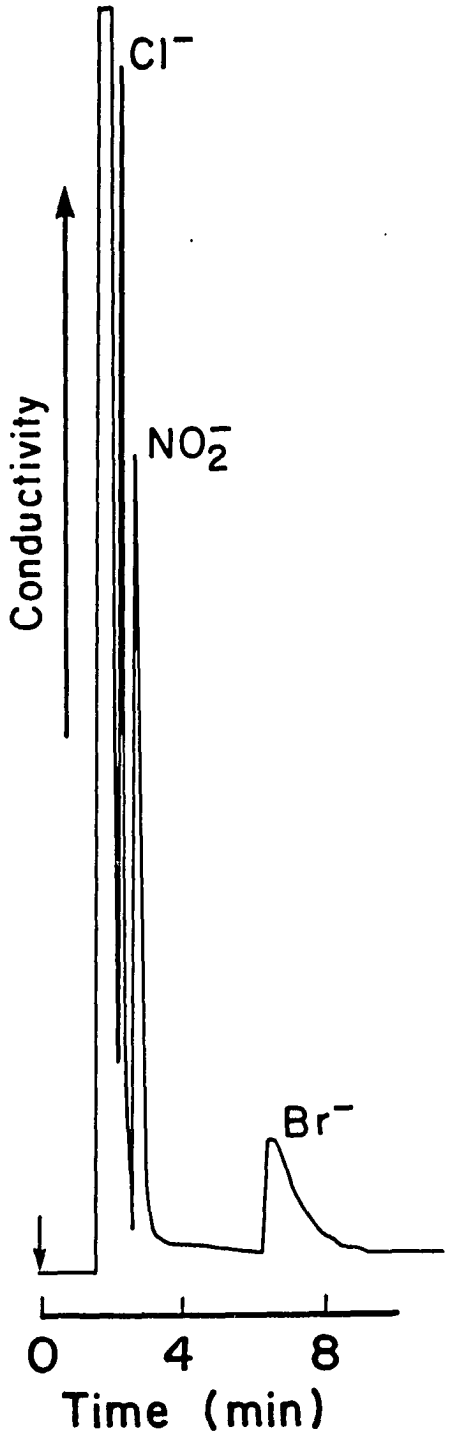
Cl⁻
NO₂⁻
Br⁻
Conductivity
0
4
8
Time (min)

columns. Figure 1 shows a separation of Cl^-, NO_2^-, and Br^- on a resin that had been prepared with 0.10 M NaCl present in the slurry. As can be seen, the Br^- peak is tailed extensively. Using the Br^- peak, this column had an efficiency of only 500 theoretical plates per meter (N/m).

A slight amount (1%) of acetonitrile was added to the slurry to alleviate the problem of latex aggregation. This also served to wet the substrate. A marked improvement in column efficiency was observed when this resin was tested chromatographically. Figure 2 shows the same separation as Figure 1, except that the resin had been prepared with 1% acetonitrile in the slurry. Even though Cl^- and NO_2^- are not well resolved under these conditions on a 15 cm column, the efficiency was 10,000 N/m. Efficiencies as high as 19,500 N/m were obtained.

Two variables that controlled the capacity were the percentage of acetonitrile present in the slurry and the amount of latex used. Figure 3 shows that, as expected, the capacity decreases as the percentage of acetonitrile increases. This is due to the fact that as the slurry becomes more hydrophobic, the latex is less readily adsorbed onto the hydrophobic substrate. It is interesting to note that while previous work indicated

Figure 2. Same separation and conditions in Figure 1. Resin was prepared in 1% acetonitrile

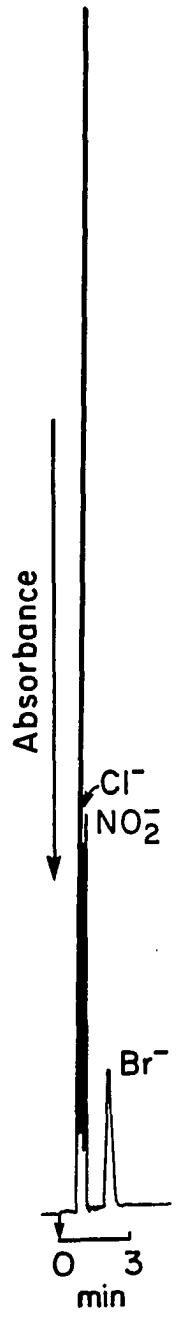
Absorbance
Cl⁻
NO₂⁻
Br⁻
0
3
min

Figure 3. Relationship between resin capacity (μeq/g) and percent acetonitrile present in slurry

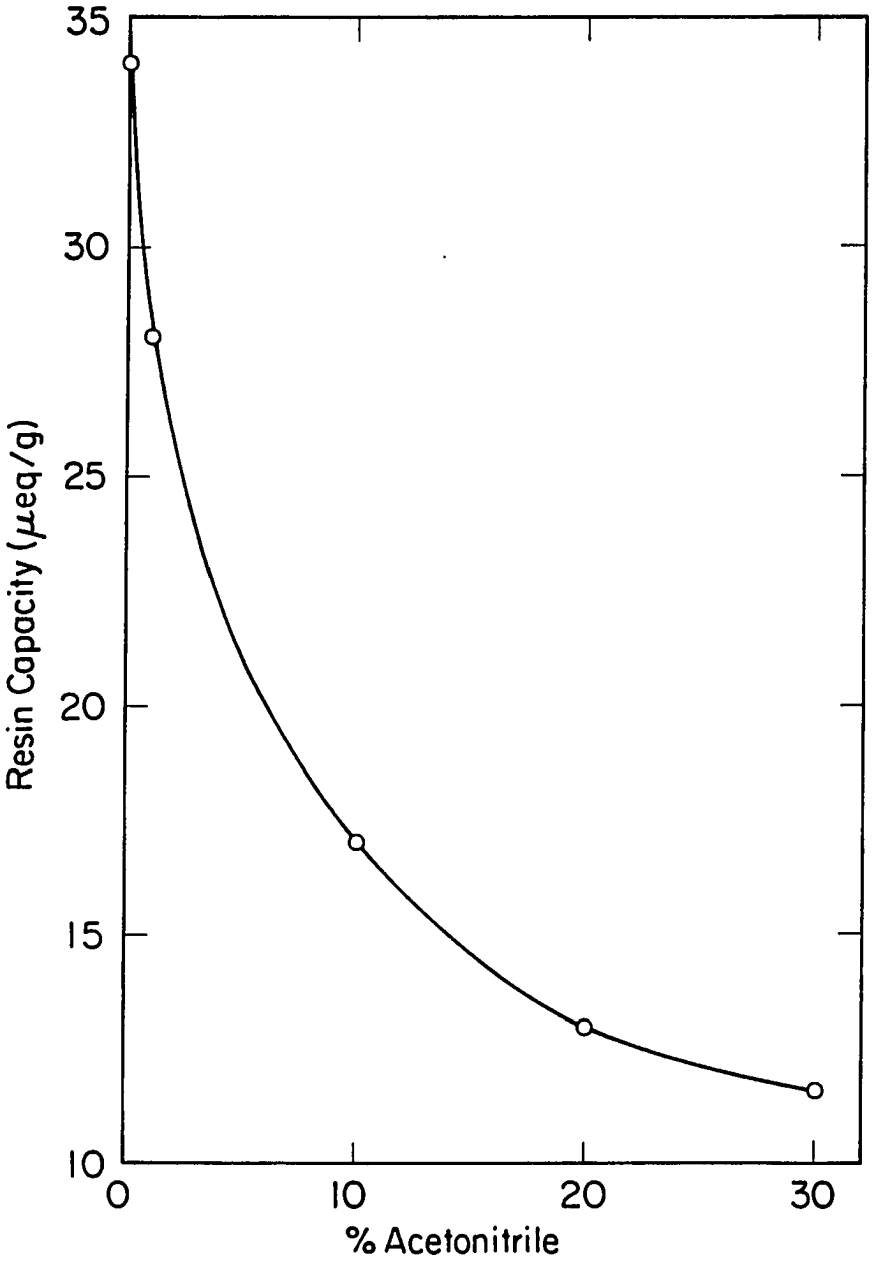
35
30
25
20
15
10
Resin Capacity (μeq/g)
0
10
20
30
% Acetonitrile

that organic modifiers washed the higher functionalized latexes off the substrate, anion-exchange resins were able to be prepared in the presence of acetonitrile using the 54% functionalized latex [11].

Figure 4 shows a nearly linear increase in capacity as the volume of latex used to coat the substrate was increased. Since this latex is more hydrophobic, a heavier coating was possible than with previous latexes. By varying the percentage of acetonitrile and the volume of latex used in the slurry, the capacity of the resin can be varied from 11.5 to 85 μeq/g.

Selectivity

Figure 5 shows the separation of seven common anions in less than seven minutes. The column is 50 x 4.6 mm i.d. Even though a short column was used, a nearly baseline separation was possible in a short analysis time. The eluent was 0.8 mM dilithium phthalate (Li_2P) at a pH value of 9.50. It is interesting to note that SO_4^{2-} and $C_2O_4^{2-}$ elute before Br-. This is unexpected since resins made with 76% functionalized latex of identical capacity did not show this elution order using a phthalate eluent [12]. One explanation for this elution order inversion is the fact that lower percent functionalized latex leaves much of the aromatic latex exposed. It has been shown that

Figure 4. Relationship between resin capacity and volume of latex added to slurry

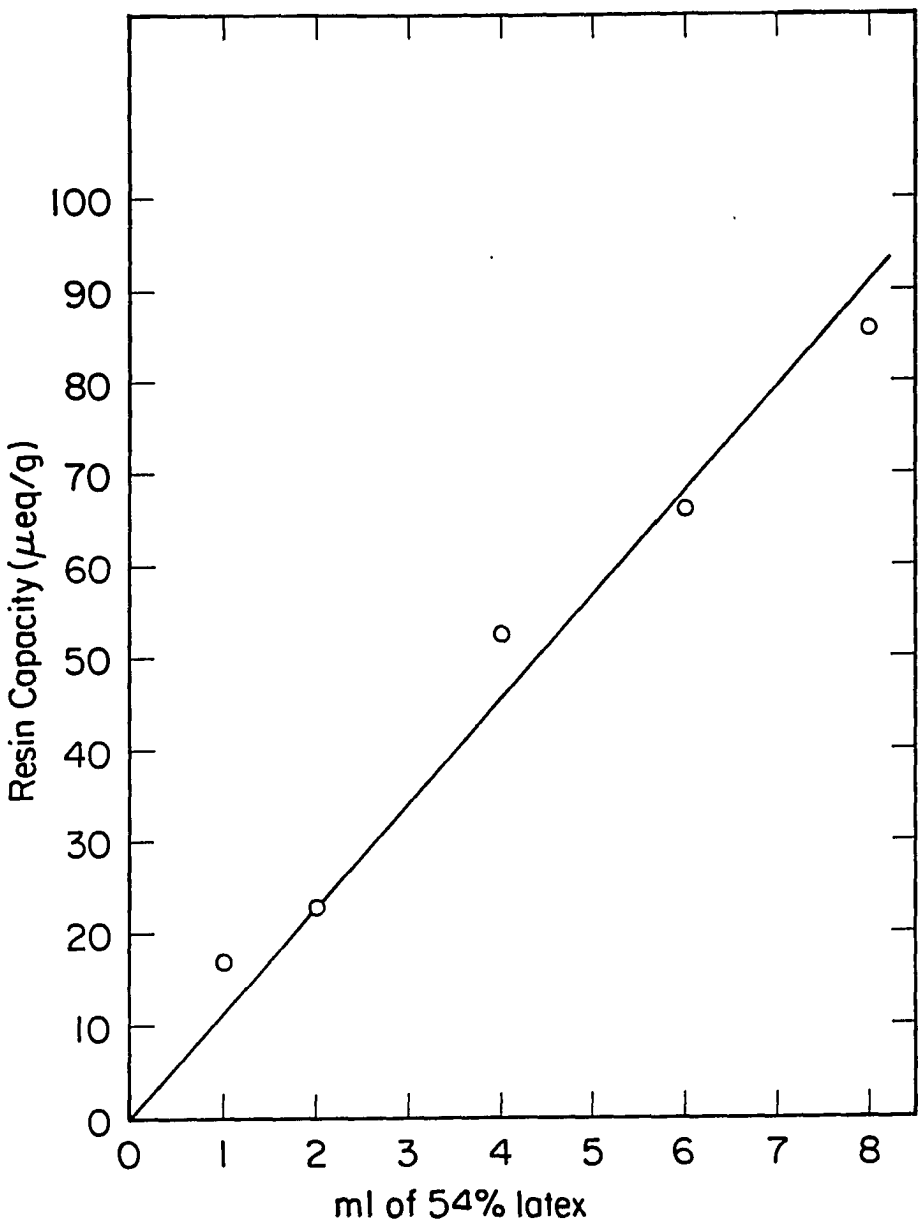
Resin Capacity (μeq/g)
100
90
80
70
60
50
40
30
20
10
0
0
1
2
3
4
5
6
7
8
ml of 54% latex

Figure 5. Separation of 5 ppm HPO_4^{2-}, 2.5 ppm Cl^-, 5 ppm NO_2^-, 10 ppm SO_4^{2-}, 10 ppm $C_2O_4^{2-}$, 20 ppm Br^-, and 30 ppm NO_3^- on a 5.0 cm x 4.6 mm i.d. column (capacity = 14.0 μeq/g). Eluent: 0.8 mM Li_2P at a pH value of 9.50. Flow rate: 1 ml/min. λ = 250 nm

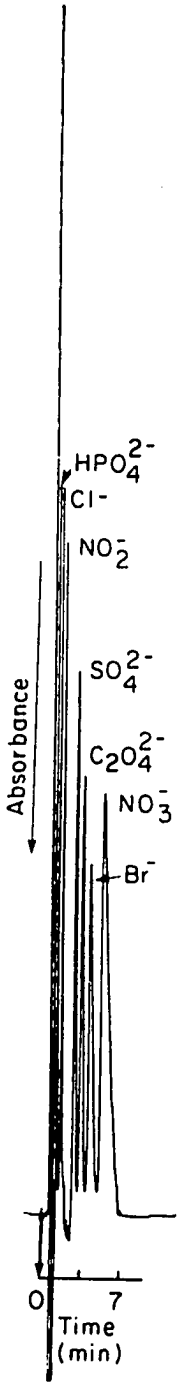
HPO_4^{2-}
Cl^-
NO_2^-
SO_4^{2-}
$C_2O_4^{2-}$
NO_3^-
Br^-
Absorbance
0
7
Time
(min)

large monovalent anions can be polarized by the π electrons of the aromatic rings, thus being slightly retained [13,14]. This would also explain why Br^- and NO_3^- are broader than expected, in spite of their short retention time.

Linda Warth showed that some ions, such as nitrate, interact with the substrate causing the chromatographic peaks to be broader [15]. By increasing the distance between the functional group and the substrate, she was able to produce sharper peaks with a decrease in retention time. A similar phenomenon may be occurring with this resin, since it has a low degree of functionalization. This would leave much of the substrate exposed and able to interact with Br^- and NO_3^- in a hydrophobic manner. To reduce this hydrophobic type interaction, methanol was added to the eluent.

The effect of adding methanol to the eluent on the elution order of the anions is seen in Table I. There is a dramatic change in the retention time of SO_4^{2-}, Br^-, and NO_3^-, while the retention time of Cl^- and NO_2^- are affected to a much smaller degree. The increase in retention time of SO_4^{2-} is probably due to the reduction of phthalate ionization in methanol. The decrease in retention times of Br^- and NO_3^- is due to either the

Table I. Effect of methanol as eluent modifier on the adjusted retention times of five common anions

% CH_3OH In Eluent	Average Adjusted retention Time (min)[a]				
	Cl^-	NO_2^-	SO_4^{2-}	Br^-	NO_3^-
0	0.62	0.99	2.93	3.64	4.60
10	0.67	1.02	3.82	3.82	4.72
20	0.66	0.96	4.53	3.57	4.53
30	0.64	0.86	5.48	3.20	3.81
40	0.61	0.76	6.47	2.78	3.22

[a]Average of three trials.

increase in hydrophobicity of the eluent or adsorbed methanol on the resin. Both would decrease the interaction between the resin and the large monovalent anions.

A commercial column (Wescan 269-029) was also used to investigate the effect of methanol on the retention times of these anions. The retention times of Cl^-, NO_2^-, Br^-, and NO_3^- were unaffected and SO_4^{2-} increased only slightly. This provides a novel dimension to latex coated resins in varying selectivity. 54% functionalized latex is also stable in the presence of methanol. After using 40% methanol in the eluent, aqueous phthalate was again used. The retention times of the anions and the elution order was essentially the same as before the use of methanol. Figure 6 shows a very nice separation of seven anions after using 40% methanol in the eluent. Two dicarboxylic acids were added to the sample.

Separation of Dicarboxylic Acids

The analysis of dicarboxylic acids is important in industries such as the wine industry. Figure 7 shows a nice separation of six dicarboxylic acids in ten minutes. As can be seen, as the alkyl chain of the dicarboxylic acids increase, the retention times of the acids decrease. This is because as the carboxylic acid moieties are

Figure 6. Separation of 10 ppm HPO_4^{2-}, 5 ppm Cl^-, 5 ppm NO_2^-, 10 ppm malonate, 20 ppm tartrate, 25 ppm SO_4^{2-}, 30 ppm Br^-, and 30 ppm NO_3^-, after 40% methanol was used as eluent modifier. Eluent: 0.5 mM Li_2P, pH value of 8.25. Flow Rate: 1 ml/min. Column: 10 cm x 4.6 mm i.d. with capacity of 35 μeq/g. λ = 270 nm

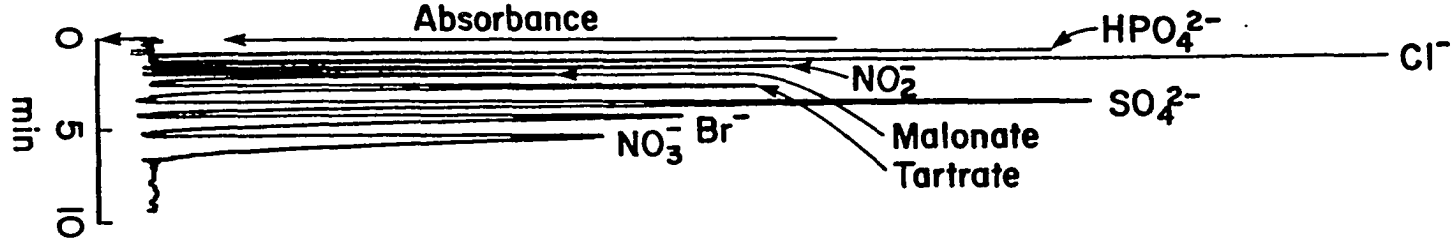
Absorbance
0
5
10
min
HPO_4^{2-}
Cl^-
NO_2^-
SO_4^{2-}
NO_3^-
Br^-
Malonate
Tartrate

Figure 7. Separation of 10 ppm glutarate, 10 ppm succinate, 10 ppm malate, 10 ppm malonate, 5 ppm tartrate, and 20 ppm oxalate on a 10 cm x 4.6 mm i.d. column (capacity = 28 μeq/g). Eluent: 0.2 mM Li_2P (pH = 8.40). λ = 245 nm)

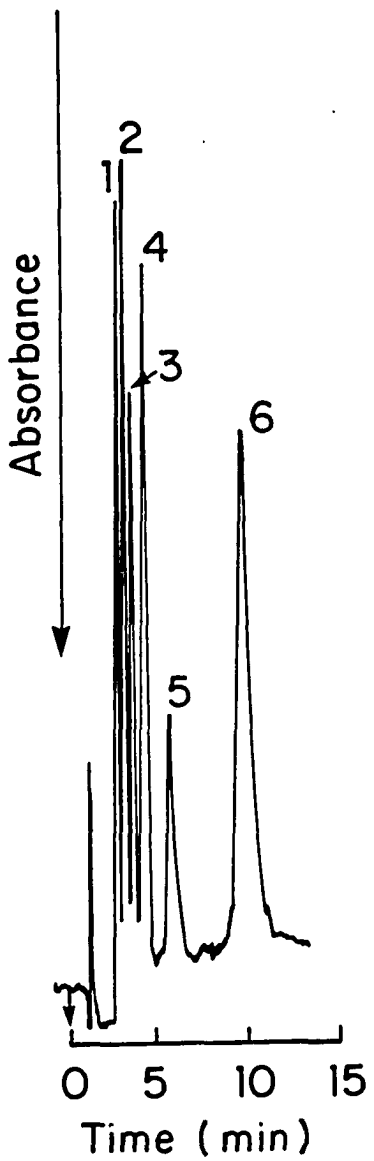
Absorbance
1
2
3
4
5
6
0
5
10
15
Time (min)

farther apart, the molecule behaves, chromatographically, similar to a monovalent anion. As the alkyl chain increases, the difference in pk_a values decreases for the straight-chain, alkyl, dicarboxylic acids. This indicates the acid groups are acting independently of each other. While the retention time of the straight-chain, alkyl, dicarboxylic acids decreases with a decrease in difference of pk_a values, this trend does not hold when other functionality, such as hydroxide groups or double bonds, is present. For example, fumarate coelutes with oxalate, and maleate coelutes with tartrate. This is the opposite elution order predicted by the difference in pk_a values: 1.41 for fumaric acid and 4.24 for maleic acid.

Indirect UV detection is the detection method of choice for analyzing dicarboxylic acids. Figure 8 shows a separation of 10 ppm each succinate, malonate, maleate, sulfate and fumarate, using 0.25 mM Li_2P at a pH value of 8.5 as the eluent with conductivity detection. As can be seen, indirect UV detection is much more sensitive.

Sensitivity and Limit of Detection

To investigate the sensitivity of this method, Cl^-, NO_3^-, and SO_4^{2-} were used. The slope of the calibration curves for these three anions was 36.6, 2.8, and 11.2 cm/ppm, respectively. Calibration curves for these three

Figure 8. Separation of 10 ppm each succinate, malonate, maleate, sulfate, and fumarate using conductivity detection (1 μSFS). Eluent: 0.25 mM Li_2P (pH = 8.50). Column same as in Figure 7

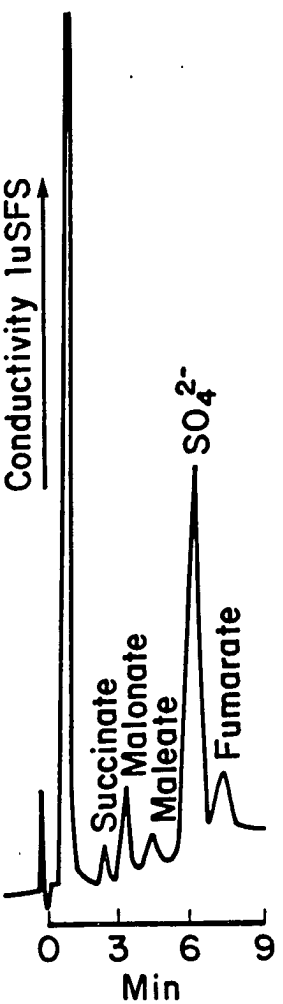
Conductivity luSFS
Succinate
Malonate
Maleate
SO_4^{2-}
Fumarate
0
3
6
9
Min

anions were linear from 0.5 to 50 ppm for Cl^- and SO_4^{2-}, and from 1.5 to 75 ppm for NO_3^-, with correlation coefficients of 0.9997 or better. This resin provides a sensitive method to quantitatively analyze anions over a very useful concentration range.

The limit of detection is also very good. Figure 9 shows the separation of 10 ppm each Cl^-, NO_2^-, SO_4^{2-}, Br^-, and 20 ppm NO_3^- in approximately seven minutes. The eluent was 0.05 mM BTA at a pH value of 4.3. The peak shape is excellent and a baseline separation was possible.

One advantage of using such a low concentration of eluent in indirect UV detection is that the baseline is very stable. The signal for these anions was well above the background, even though only 10 μl of sample was injected.

Figure 10 shows a similar separation as Figure 9, except that conductivity was used as the method of detection. Li_2P was again used as the eluent, but at a pH value of 6.00. A comparison between Figures 9 and 10 indicates that indirect UV detection may provide lower limits of detection.

This resin also produced quite efficient separations. For example, Figure 11 is the separation of seven anions in less than six minutes. Using the sulfate peak to

Figure 9. Separation of 10 ppm Cl^-, 10 ppm NO_2^-, 10 ppm SO_4^{2-}, 10 ppm Br^-, and 20 ppm NO_3^- on 5 cm x 4.6 mm i.d. column (capacity = 27 μeq/g). Eluent: 0.05 mM BTA (pH = 4.3). Flow rate: 1 ml/min. λ = 250 nm

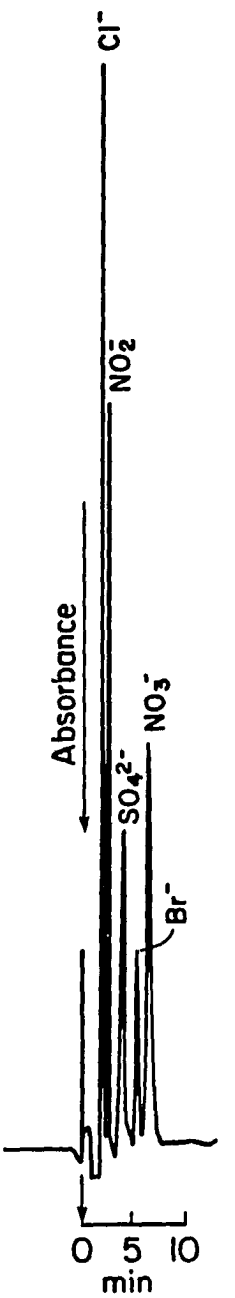
Cl⁻
NO₂⁻
Absorbance
NO₃⁻
SO₄²⁻
Br⁻
0 5 10
min

Figure 10. Separation of 10 ppm Cl^-, 10 ppm NO_2^-, 10 ppm SO_4^{2-}, 30 ppm Br^-, and 20 ppm NO_3^- on same column as Figure 9. Eluent: 1.0 mM Li_2P (pH = 6.00). Flow rate: 1 ml/min. Conductivity detection: 1 μSFS

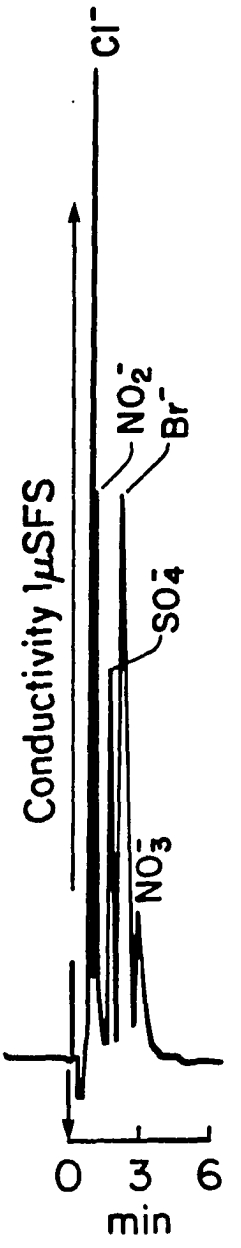
Cl⁻
NO₂⁻
Br⁻
SO₄⁻
NO₃⁻
Conductivity 1μSFS
0
3
6
min

Figure 11. Separation of 5 ppm HPO_4^{2-}, 5 ppm Cl^-, 12 ppm succinate, 10 ppm malonate, 10 ppm tartrate, 6 ppm SO_4^{2-}, and 20 ppm $C_2O_4^{2-}$, in order of elution, on a 5cm x 4.6 mm i.d. column (capacity = 16 μeq/g). Eluent: 0.5 mM Li_2P (pH = 9.00). Flow rate: 0.75 ml/min. λ = 270 nm

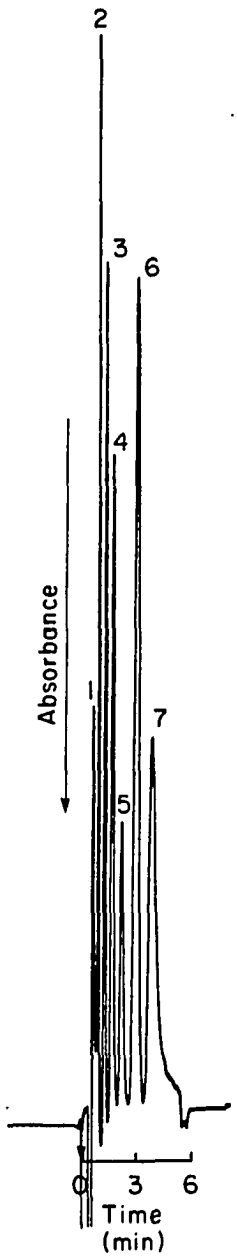
2
3
6
4
Absorbance
7
5
0
3
6
Time
(min)

calculate the efficiency, this column had an efficiency of 19500 N/m.

Finally, Figure 12 demonstrates a practical application for this resin: rapid analysis of NO_3^-. Cl^- and SO_4^{2-} elute very early (Cl^- elutes in the injection peak) and NO_3^- elutes in about 2.5 minutes. A 10 μl injection of 5 ppm (or 50 ng) of SO_4^{2-}, Br^-, and NO_3^- were injected. As can be seen, this resin provides a very rapid method to analyze low concentrations of NO_3^-.

Figure 12. Rapid separation of 5 ppm each SO_4^{2-}, Br^-, and NO_3^- on a 5.0 cm x 4.6 mm i.d. column (capacity = 15 μeq/g). Eluent: 0.05 mM BTA (pH = 4.6). Flow rate: 1 ml/min. λ = 240 nm

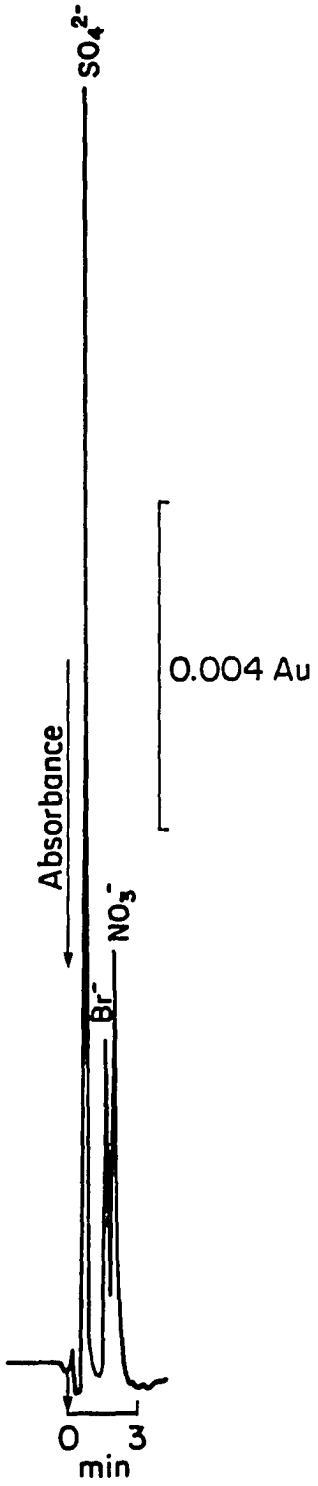
SO_4^{2-}
0.004 Au
Absorbance
NO_3^-
Br^-
0
3
min

CONCLUSION

It has been demonstrated in this work that resins prepared by coating small, non-porous, spherical, polystyrene beads with anion-exchanging latexes offer several advantages over other types of anion-exchange resins.

First, these resins can be prepared quickly and safely. The preparation time is typically only one hour, without producing any carcinogenic by-products.

Second, the capacity of these resins can be easily controlled by varying the percentage of acetonitrile or the volume of latex present during mixing. A capacity range of 14 to 85 μeq/g is obtainable, which is a very useful range in SCIC.

Third, using 54% functionalized latex, this resin possesses a unique and useful selectivity. For example, with the inherent SO_4^{2-}/NO_3^- inversion, a rapid NO_3^- analysis is possible without interference from Cl^- or SO_4^{2-}. This eliminates the need to wait for SO_4^{2-} to elute before another NO_3^- analysis is begun.

Finally, because of the low capacity, high efficiency, and selectivity of this resin, short columns and dilute eluents can be used to perform analyses of mixtures of

inorganic anions and dicarboxylic acids. The result is an increase in sensitivity and a decrease in the limits of detection.

REFERENCES

1. Small, H.; Stevens, T. S.; Bauman, W. C. Anal. Chem. 1975, 47, 1801.

2. Gjerde, D. T.; Fritz, J. S.; Schmuckler, G. J. Chromatogr. 1979, 186, 509.

3. Small, H.; Stevens, T. U.S. Patent 4 101 460.

4. Stevens, T. S.; Langhorst, M. A. Anal. Chem. 1982, 54, 950.

5. Barron, R. E.; Fritz, F. S. React. Polymers 1983, 1, 215.

6. Cassidy, R. M.; Elchuk, S. J. Chromatogr. 1983, 262, 311.

7. Bidlingmeyer, B. A. J. Chromatogr. Sci. 1980, 18, 525.

8. DuVal, D. L.; Fritz, J. S. J. Chromatogr. 1984, 295, 89.

9. Al-Omair, A. S.; Lyle, S. J. Talanta 1987, 43, 361.

10. Wheals, B. B. J. Chromatogr. 1987, 402, 115.

11. Warth, L. M.; Fritz, J. S.; Naples, J. O. J. Chromatogr. 1989, 462, 165.

12. Miura, Y.; Fritz, J. S. J. Chromatogr. 1989, 482, 155.

13. Afrashtehfar, S.; Cantwell, F. F. Anal. Chem. 1982, 54, 2422.

14. Cantwell, F. F.; Puon, S. Anal. Chem. 1979, 51, 623.

15. Warth, L. M.; Fritz, J. S. J. Chromatogr. Sci. 1988, 26, 630.

GENERAL CONCLUSION

Causes of band broadening in capillary, gas chromatography were investigated. Using the Golay equation, it was shown that the presence of a diluent significantly increased the extra-column variance, in early eluting peaks, when a liquid injection was used. The cause of this phenomenon was also discussed.

A mathematical method based on an iterative method was developed to obtain the correct hold-up time of a capillary column using a flame ionization detector. This method took advantage of the programmable ability of a common, hand-held calculator. Also discussed were the application of this method for calculating Kovats indices and the calculation of capacity factors.

The injection peak in single-column, anion exchange chromatography was used to quantitatively determine simple mixtures of cations in solution. By preparing the sample so that it contains the same concentration and pH value of eluent ions as the mobile phase, it was shown that the injection peak area was proportional to the concentration of cations and dependent on the type of cation present. Binary mixtures of salts in the presence of moderate amounts of acid or base could be quantitated by the

combination of information from injection and sample peak areas.

A new, low capacity, anion-exchange resin was developed which possessed a unique selectivity for sulfate and oxalate over bromide and nitrate. This low capacity resin made it possible to separate dicarboxylic acids without interference from inorganic ions. The selectivity was shown to be caused by interactions between the resin matrix and large monovalent anions. This resin also made it possible to use very short columns, which reduced the analysis time for many anions. The efficiency of this resin was shown to be quite good.

ACKNOWLEDGMENTS

This research was partially funded by Rohm & Haas of Philadelphia. I especially appreciate the advice and support of Dr. John O. Naples, at Rohm & Haas, during my last two years at Iowa State University.

This work was performed at Ames Laboratory under contract no. W-7405-eng-82 with the U. S. Department of Energy. The United States government has assigned the DOE Report number IS-T-1467 to this thesis.

I would like to thank Dr. James S. Fritz for his support and guidance. I appreciate the freedom he provided and the high expectations he required.

I would also like to thank two collaborators, Dr. Dan Scott and Dr. Gabriella Schmuckler. Dr. Dan Scott's contributions and discussions on Section II were invaluable. Dr. Gabriella Schmuckler and I worked very closely on Section III. The experience and friendship obtained by working with Dr. Schmuckler were priceless.

My colleagues at Iowa State University have been an asset to my career. The discussions we have had have been most helpful. I especially thank Mark Main. His friendship has made my work here much more enjoyable. I wish him the best of luck in his new career.

Three people who helped make this thesis possible are my parents, Frances Strasburg and Beverly and Eldon Himsel. Their support and belief in me were a constant source of strength.

Finally, I thank my wife, Beth, and our two sons, Chris and Josh. Their sacrificial love, patience, and encouragement have made this work a reality.